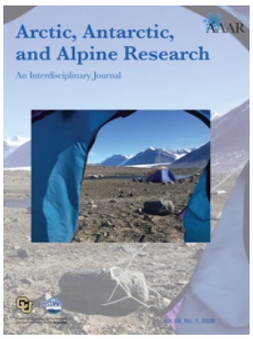

Taylor & Francis
Taylor & Francis Group

Arctic, Antarctic, and Alpine Research

An Interdisciplinary Journal

ISSN: 1523-0430 (Print) 1938-4246 (Online) Journal homepage: www.tandfonline.com/journals/uaar20

Beringian flora and fauna from *sed*aDNA at Duvanny Yar, Sakha Republic, during marine isotope stages 2 and 3

Mary Edwards, Julian Murton, Min Huang, Alistair Monteath, Anatoly Lozhkin, Yulia Korzun & Yucheng Wang

To cite this article: Mary Edwards, Julian Murton, Min Huang, Alistair Monteath, Anatoly Lozhkin, Yulia Korzun & Yucheng Wang (2026) Beringian flora and fauna from *sed*aDNA at Duvanny Yar, Sakha Republic, during marine isotope stages 2 and 3, Arctic, Antarctic, and Alpine Research, 58:1, 2593677, DOI: 10.1080/15230430.2025.2593677

To link to this article: https://doi.org/10.1080/15230430.2025.2593677

ARCTIC, ANTARCTIC, AND ALPINE RESEARCH
2026, VOL. 58, NO. 1, 2593677
https://doi.org/10.1080/15230430.2025.2593677

Taylor & Francis
Taylor & Francis Group

Beringian flora and fauna from *sed*aDNA at Duvanny Yar, Sakha Republic, during marine isotope stages 2 and 3

Mary Edwards[a], Julian Murton[b], Min Huang[c,d], Alistair Monteath[e], Anatoly Lozhkin[f], Yulia Korzun[f], and Yucheng Wang[c,g,h]

[a]School of Geography and Environmental Science, University of Southampton, Southampton, UK; [b]Department of Geography, University of Sussex, Brighton, UK; [c]Group of Alpine Paleoecology and Human Adaptation (ALPHA), State Key Laboratory of Tibetan Plateau Earth System, Environment and Resources (TPESRE), Institute of Tibetan Plateau Research, Chinese Academy of Sciences, Beijing, China; [d]MOE Key Laboratory of Western China's Environmental System, College of Earth and Environmental Sciences, Lanzhou University, Lanzhou, China; [e]British Antarctic Survey, Cambridge, UK; [f]North-East Interdisciplinary Scientific Research Institute, Magadan, Russia; [g]Department of Genetics, University of Cambridge, Cambridge, UK; [h]Centre for Ancient Environmental Genomics, Globe Institute, University of Copenhagen, Copenhagen, Denmark

ABSTRACT

Beringia's extensive late Quaternary deposits of yedoma silt provide rich floristic and faunal records. Sampling of frozen yedoma exposures typically uses multiple baydzherakhs (residual silt heaps developed as conical thermokarst mounds) that collectively straddle vertical and horizontal space in thaw slumps. We used radiocarbon-dated vertical and horizontal transects to assess stratigraphic and sampling consistency at Duvanny Yar (a critical late Pleistocene stratotype). Most samples are ascribed to later marine isotope stage (MIS) 3 or to MIS 2 (ca. 40,000 to 20,000 years ago). The horizontal (MIS 3) transect revealed an undulating paleolandscape. Sedimentary ancient DNA (*sed*aDNA) from frozen yedoma revealed floristic composition in time and space. Metabarcoding and shotgun metagenomic molecular floras and pollen spectra are ecologically consistent. Floristically, little separates MIS 3 and 2; xeric, treeless vegetation, dominated by grasses and forbs including disturbance indicators, characterizes both stages. Holocene samples have a distinct, woody-dominated flora. Ordination of metabarcoding samples from the horizontal transect shows samples are highly variable but do not form a discernible spatial gradient or mosaic, possibly reflecting microtopographically driven plant distribution across a largely homogeneous landscape. Mammals identified from MIS 3 and 2 include horse, steppe bison, woolly rhinoceros, woolly mammoth, reindeer, hare, and vole.

ARTICLE HISTORY
Received 3 March 2025
Revised 7 October 2025
Accepted 12 November 2025

KEYWORDS
Beringia; metabarcoding; pollen; *sed*aDNA; shotgun metagenomics

Introduction

The Yedoma Ice Complex of the unglaciated lowlands of northeast Siberia and Chukotka formed during cold phases of the Late Pleistocene as landscapes were draped with sediment, largely through eolian deposition, though other processes, such as colluviation and fluvial deposition, also contributed (see reviews in Murton et al. 2015; Péwé and Journaux 1983; Strauss et al. 2012; Schirrmeister et al. 2020, 2025). The land surface can be raised by tens of meters during a glacial cycle, and under conditions of severe cold, syngenetic ice wedges grew apace with sediment deposition. The result is a deposit (ice complex) formed of silt and large amounts of ice (up to 63 percent by volume; Ulrich et al. 2014) that may remain perennially frozen for many millennia and is characterized by incipient—and occasionally clearly identifiable—paleosols (Gubin 2002, cited in Murton et al., 2015; Lupachev et al. 2025). Yedoma exposures across Beringia have yielded important paleobiological evidence, including numerous skeletal remains of the Pleistocene mammalian fauna and, occasionally, spectacular frozen mummies (e.g., Guthrie 1990; Lozhkin and Anderson 2016; Boeskorov et al. 2018), as well as invertebrates, pollen and plant macrofossils (e.g., Sher et al. 2005; Monteath et al. 2023).

Detailed examination shows that the frozen sediments are enriched in fine plant detritus (Gubin and Veremeeva 2010), providing a promising substrate for the retrieval of plant *sed*aDNA. Indeed, in recent

CONTACT Mary Edwards m.e.edwards@soton.ac.uk School of Geography and Environmental Science, University of Southampton, University Road, Southampton SO17 1BJ, UK
Supplemental data for this article can be accessed online at https://doi.org/10.1080/15230430.2025.2593677

decades, ancient DNA from fossils and the sediment itself has provided extensive new insights about a range of components of past northern ecosystems (particularly east and west Beringia), including plants, vertebrates, fungi, and bacteria/archaea (Willerslev et al. 2003; Arnold et al. 2011; Epp et al. 2012; Zimmermann et al. 2017, 2019; Wang et al. 2021; Murchie et al. 2021a, 2023; Courtin et al. 2022; Seeber et al. 2024).

Duvanny Yar comprises a series of yedoma exposures along 10–12 km of the east bank of the Kolyma River in Yakutia, northeast Siberia (Figure 1). Here, the Kolyma cuts through sediments of Middle and Late Pleistocene age. The 1979 Tour Guide for the 14th Pacific Science Congress (Sher et al. 1979) summarizes the report of Kaplina (1978); this excursion and document were probably the first introduction for Western scientists to Duvanny Yar. The locality has been particularly well studied; it is the stratotype for the "yedoma suite" of northeast Siberia for the Middle-to-Late Pleistocene (Kaplina et al. 1978), and its name was used by Hopkins (1982) to describe the widespread, cold, dry full-glacial interval experienced across Beringia (broadly equivalent to MIS 2). Recent studies have detailed macrofossils from rodent burrows (Zanina et al. 2011)

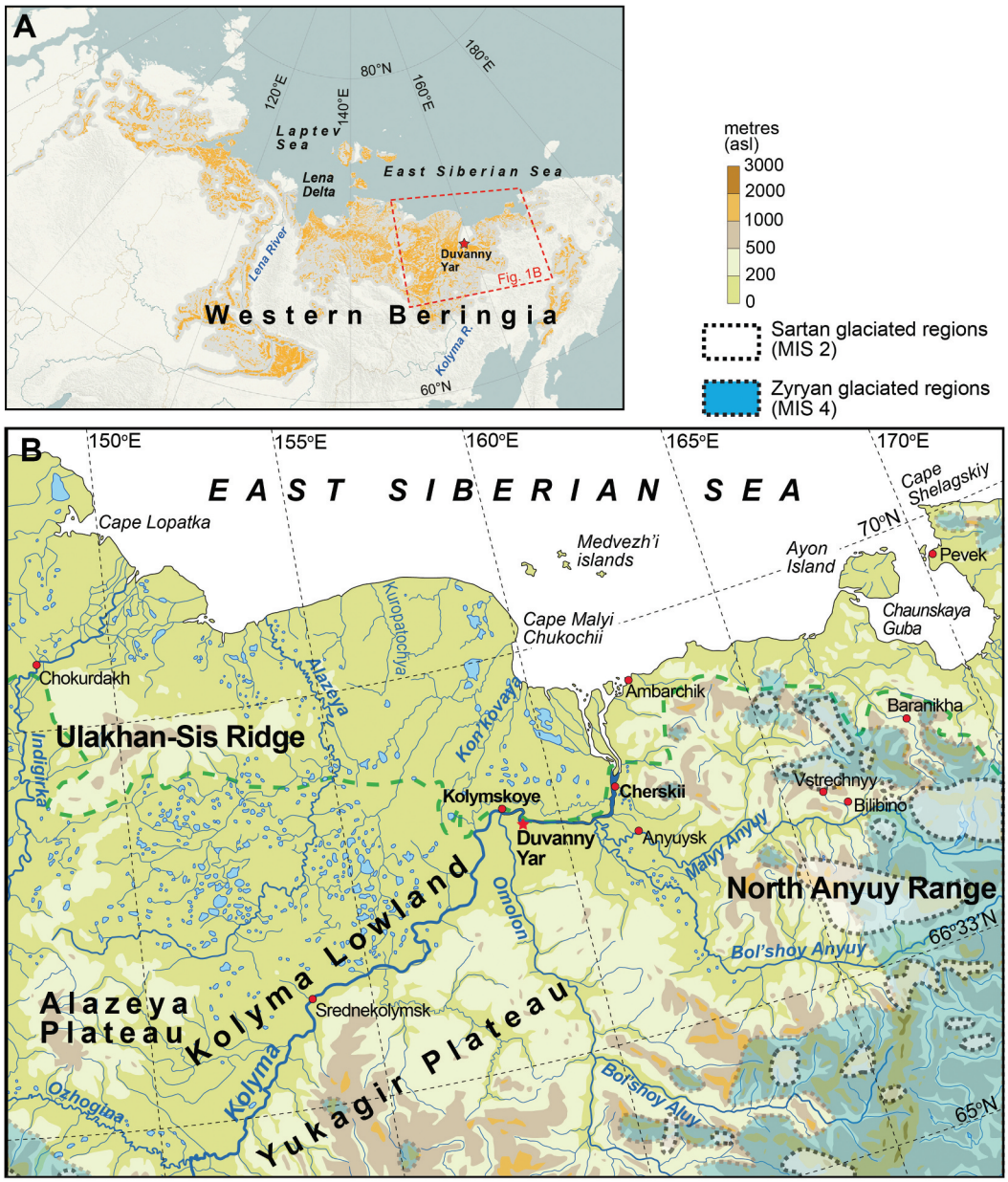

Figure 1. (A): Map of yedoma distribution in northeast Siberia. Grey area denotes yedoma domain, and Orange area denotes yedoma deposits. (B): Location of the Duvanny Yar exposure. (A) Modified from Strauss, Laboor, and Schirrmeister et al. (2021). Legend on right side of (A) refers to elevations above sea level (asl) shown in (B). (B) Modified from Murton et al. (2015).

and paleosol development (e.g., Gubin and Verameeva, 2010); for a summary of research at the site, see Murton et al. (2015).

The site was the focus of intensive sampling in 2009 as part of the EU project EcoChange (Willerslev et al. 2014). Murton et al. (2015) provided a comprehensive view of the physical properties and evolution of the deposits at Duvanny Yar (including sedimentology, chronology, ice and permafrost properties, geochemistry and pollen), but the *sed*aDNA data have to date only featured in larger data syntheses and have not been examined in detail. Drawing on detailed stratigraphic and chronological documentation of the 2009 exposure, this study addresses the detailed *sed*aDNA record, asking both methodological and paleoecological questions: how uncertainties in dating and depositional patterns affect the realistic temporal resolution of proxy records from yedoma, how records of *sed*aDNA derived from metabarcoding and shotgun metagenomics compare, and what, together with fossil pollen, they tell us about this herbivore-dominated ecosystem during the latter part of MIS 3 (ca. 39,000–30,000 cal yr BP), and the following full-glacial interval (MIS 2; ca. 30,000–20,000 cal yr BP) in the lower Kolyma region.

The challenges of yedoma sampling

The physical study of yedoma exposures is particularly challenging. Other than directly drilling from the surface (e.g., Zimmermann et al. 2017; Lupachev et al. 2025), deposits are only accessible when they are exposed to air, and thus to thaw in summer or sublimation in winter. In NE Siberia and Chukotka, exposures typically comprise sediment remnants left after ice-wedge melting, which take the form of pyramidal heaps of sediment known as baydzherakhs—a type of thermokarst mound. Older baydzherakhs lie lower down on the slump floor and farther from the thawing face, and thus a temporal reconstruction has both vertical and horizontal components, unlike a conventional sediment core or a sampled near-vertical face. It has occasionally been possible to sample the vertical upper wall of exposures using climbing equipment (e.g., Wetterich et al. 2014), but in other cases reconstructions still rely on correlation across sets of baydzherakhs. These constraints can limit the temporal and spatial precision of reconstructions based on yedoma sediment and require extensive dating and careful interpretation of data (see, for example, Sher et al. 2005).

In 2009, Duvanny Yar was sampled for *sed*aDNA during a detailed sedimentological study of one of its large exposures (see Murton et al., 2015; Willerslev et al. 2014). Many of the ca. 130 sediment samples taken have an associated radiocarbon date. As well as building a vertical profile from a set of sections derived from multiple baydzherakhs and part of the headwall of the exposure (Figure S1), we made a horizontal traverse of five baydzherakhs, creating, in effect, a three-dimensional series of individually dated samples that date to MIS 3. Even apparently "flat" landscapes—ancient as well as modern—usually reveal some topographic variation that can contribute to soil and vegetation mosaics. The potential for spatial variation means that single vertical profiles can intercept changes in deposits that could be either regional or local. Such ambiguity risks reconstructing an inaccurate picture of environmental variation (see Sher et al. 2005 for a detailed discussion of this problem); thus, variation in paleodata from a horizontal transect of baydzherakhs may reveal differences in space, as well as in time.

Temporal heterogeneity across vertical yedoma sequences

Our first aim was to test the assumption that vertically correlated samples would be coeval across a horizontal section, which underlies the conventional construction of paleorecords from baydzherakh sequences. Dating such deposits is challenging. With increasing age, the presence of small amounts of anachronously young material presents an increasing risk of dates being too young (Sher et al. 2005; Monteath et al. 2025). Second, the dating errors become unavoidably large with increasing age, decreasing temporal resolution. Arguably, to test the assumption, dating of (virtually) every sample is required to constrain the potential spatiotemporal uncertainties; we were able to use the exceptional radiocarbon record from the site (Poznan Radiocarbon Laboratory; see Murton et al. 2015; Willerslev et al. 2014) to trace ancient surfaces across time and two-dimensional space.

What does a plant sedaDNA sample from ancient yedoma represent?

The taphonomy of *sed*aDNA (its sources, and how it becomes integrated in soil or associated with a sediment matrix; e.g., Giguet-Covex et al. 2019; Freeman et al. 2023) and the representation by *sed*aDNA of vegetation are important considerations. Source areas in lake sediments reflect vegetation in the hydrologic catchment (e.g., Alsos et al. 2018). For modern vegetation communities and associated soil in north Norway, Yoccoz et al. (2012) demonstrated a close match of plant taxa and *sed*aDNA. Edwards et al. (2018) showed for Svalbard tundra that the taxonomic composition of modern soil

*sed*aDNA has high fidelity with overlying vegetation, but strongly under-samples any area greater than ca. 1 m^2. In both lacustrine and terrestrial environments, there is little evidence of contamination from pollen-derived aDNA or long-distance *sed*aDNA transport.

These observations suggest that taking one sample at each time-point—as is often done to obtain a vertical time series—while likely to be floristically accurate, offers a somewhat restricted view of the local flora. For a transect across a given temporal horizon we should detect more taxa in the local species pool as the number of samples across the paleo-surface increases and thus obtain an estimate of how completely *sed*aDNA can sample the local vegetation; we can then address the following questions: i) how many samples does it take to detect all identified taxa across a transect of a given age, and ii) can we detect any part of a local-scale mosaic on the Duvanny Yar paleo-landscape, if it existed?

How does methodology affect sedaDNA retrieval and resultant floras?

Given the availability of a newer shotgun metagenomic (hereafter, shotgun) dataset based on a subset of original samples (Wang et al. 2021), we can compare the metabarcoding taxon richness and composition with the metagenomic data from the same samples within a stratigraphic context to resolve several methodological issues. Importantly, we can test the sensitivity of metabarcoding and shotgun in detecting different taxa and explore the potential reasons resulting in these differences: i) assessment and reduction of polymerase chain reaction (PCR) biases and the relatively few PCR repeats used in the original metabarcoding study; ii) testing whether the *sed*aDNA is truly ancient by assessing molecular damage patterns; iii) checking for bias in the metabarcoding data due to use of internal transcribed spacer (ITS) nuclear primers, which favor grasses, Asteraceae and Salicaceae, and because most Salicaceae molecular taxonomic units (MOTUs) were excluded from the metabarcoding data as they appeared in sequencing blanks. On the other hand, estimation of taxonomic richness based on shotgun data is also affected by sources of bias, for example, the availability and completeness of reference genomes, and the genetic divergence of a target taxon from other organisms. In both approaches, the relation of read number to abundance (i.e., biomass) is uncertain, though it seems likely that major trends in read abundance reflect aspects of plant abundance. We visit these methodological issues here, but they deserve further exploration elsewhere.

SedaDNA vs pollen

Pollen from terrestrial deposits samples both a regional, wind-blown component (that is probably somewhat homogeneous) and a local component derived from plants at the site (Jacobsen and Bradshaw 1981; Prentice 1985), whereas the *sed*aDNA source from soil is local (see above). Thus, pollen and *sed*aDNA records from the same deposit are worth comparing, as they provide partly different, partly overlapping floras (Jorgensen et al. 2012; Zimmermann et al. 2017; Edwards et al. 2018; Parducci et al. 2019). We compared the *sed*aDNA record with the pollen record published in Murton et al., (2015) and pollen from the horizontal transect.

The sedaDNA mammal fauna

While mammalian DNA was not recovered from Duvanny Yar in a pioneering metabarcoding study (Boessenkool et al. 2012), it was obtained in this study via shotgun sequencing. It provides information on faunal composition through time for the site and can be compared with several bone databases available for the region (e.g., Sher et al. 2005).

The nature of late-Pleistocene vegetation in NE Siberia

The Beringian vegetation that was widespread during cold stages of the Pleistocene, and which formed the forage of the megafauna (defined by Martin 1984 as animals weighing ≥44 kg), has been conceptualized in different ways, often reflecting whether the focus is the mammals or the plants they ate. Botanically, the term "steppe–tundra" captures well the widely observed mix of steppe and tundra taxa. Suggested modern analogues include sparse "cryoxeric" steppe in west Beringia (Yurtsev, 1982), high-elevation steppe and tundra in central Asia (Chytrý et al. 2019), and boreal steppe merging into dry tundra on an elevational gradient in east Beringia (Edwards and Armbruster 1989). Pollen data indicate vegetation cover was virtually treeless and dominated by graminoids and forbs (*Artemisia* often dominant, with lower values of other forbs; Sher et al. 2005; Andreev et al. 2011). More recent metabarcoding-based *sed*aDNA results from northern localities differ from pollen records in emphasizing a far greater abundance and/or variety of diverse forbs

(e.g., Willerslev et al. 2014; Clarke et al. 2019, 2024; Murchie et al. 2021a). Shotgun *sed*aDNA data (Wang et al. 2021) suggested a balanced composition of forbs and graminoids. The higher overall floral diversity of the *sed*aDNA floras improves upon traditional pollen-based floristic information and can be used to create enhanced floristic lists and inform on community composition and functional dominance (Willerslev et al. 2014; Clarke et al. 2024).

Geographic setting

The locality studied at Duvanny Yar (68°, 37′, 51.1″N; 159°, 09′, 06.8″E; Figures 1 and 2) is a large, retrogressive thaw slump that was active in 2009. It exposed ca. 40 vertical meters of deposits from river level to the land surface above the headwall (Figure 2). Sediments probably relating to MIS 5 (the last interglaciation) are visible at the base in some localities, overlain by sediments from MIS stages 4–2 and a Holocene soil. The uppermost several meters comprise ice-rich sediments of a "transition zone" (i.e. an ice-rich transient layer above an even icier intermediate layer; Shur, Hinkel, and Nelson 2005; reviewed in Murton 2022a, 2022b) that have previously thawed and are now refrozen beneath the modern active layer and above the top of Pleistocene permafrost (Gubin and Lupachev 2008).

The present-day climate of the Kolyma Lowland is cold continental. Interpolated mean annual air temperature is ca. −14°C (−11°C at Cherskiy; Figure 1). Mean July temperature at Kolymskoye (Figure 1) is 10.9°C; mean January temperature is −34.8°C. Mean annual precipitation (MAP) is ≤ 200 mm, mostly falling during the summer (~39 percent) and fall (~31 percent). Snow cover generally persists from September to May (data from Sher et al. 1979; Park et al. 2008; Murton et al., 2015, Vasil'chuk and Budantseva, 2022).

Duvanny Yar lies near the northern boreal treeline. Open larch (*Larix dahurica*) forest characterizes the site, with a shrub understorey of birch (*Betula middendorfii*) and willow (*Salix* spp.). Northward, and at higher elevation, the vegetation grades into forest–tundra with *Larix* and the shrub pine, *Pinus pumila*. Soils (gelisols, cryosols) are subject to frost action, and organic layers tend to be shallow (i.e., <40 cm; Smith et al. 1995). The thickness of the modern active layer is ~30–40 cm beneath peaty deposits in alases, ~40–50 cm under earth hummocks formed on the upland yedoma surface, and ~80 cm on the Kolyma River's active silty floodplain (Smith et al. 1995). A thickness of ~30-40 cm was recorded by Murton et al. (2015, Figure 16 therein) beneath an organic layer of 25–60 cm on the yedoma upland surface at Duvanny Yar.

Figure 2. Syngenetic ice-wedge ice (shiny) and yedoma silt (dark gray) that form the Yedoma Ice Complex at Duvanny Yar. The wedge ice melts out between columns of frozen silt, leaving conical thermokarst mounds of silt (baydzherakhs). People for scale.

Methods

Field work

Field work took place in the summer of 2009: details of description and sampling approaches are reported in Murton et al. (2015) for the main studied (vertical) section at Duvanny Yar (Figure S1). Additionally, we chose a group of five baydzherakhs that stood at approximately the same height on the exposure, forming a transect that was carefully sighted into a datum so that the heights and horizontal distances between samples could be calculated (heights given in relation to river level at the time of sampling). For this transect, samples were taken in the arrangement shown in Figure 3. The face was cleaned back, and frozen material was collected for analysis of sediment, pollen, and *sed*aDNA, the latter following the protocol described in Willerslev et al. (2014), whereby each *sed*aDNA sample was collected with instruments sterilized with bleach and remained frozen. Non-DNA samples were double-bagged using new, sealable plastic bags; DNA samples were bagged, sealed and transferred as soon as possible to a portable freezer. Duplicate samples were also collected for radiocarbon dating (see Murton et al., 2015; Willerslev et al. 2014).

Dating

Frozen samples were thawed and wet-sieved at Cherskii Field Station. Sieved material, dominated by fine roots, was AMS radiocarbon-dated at Adam Mickiewicz

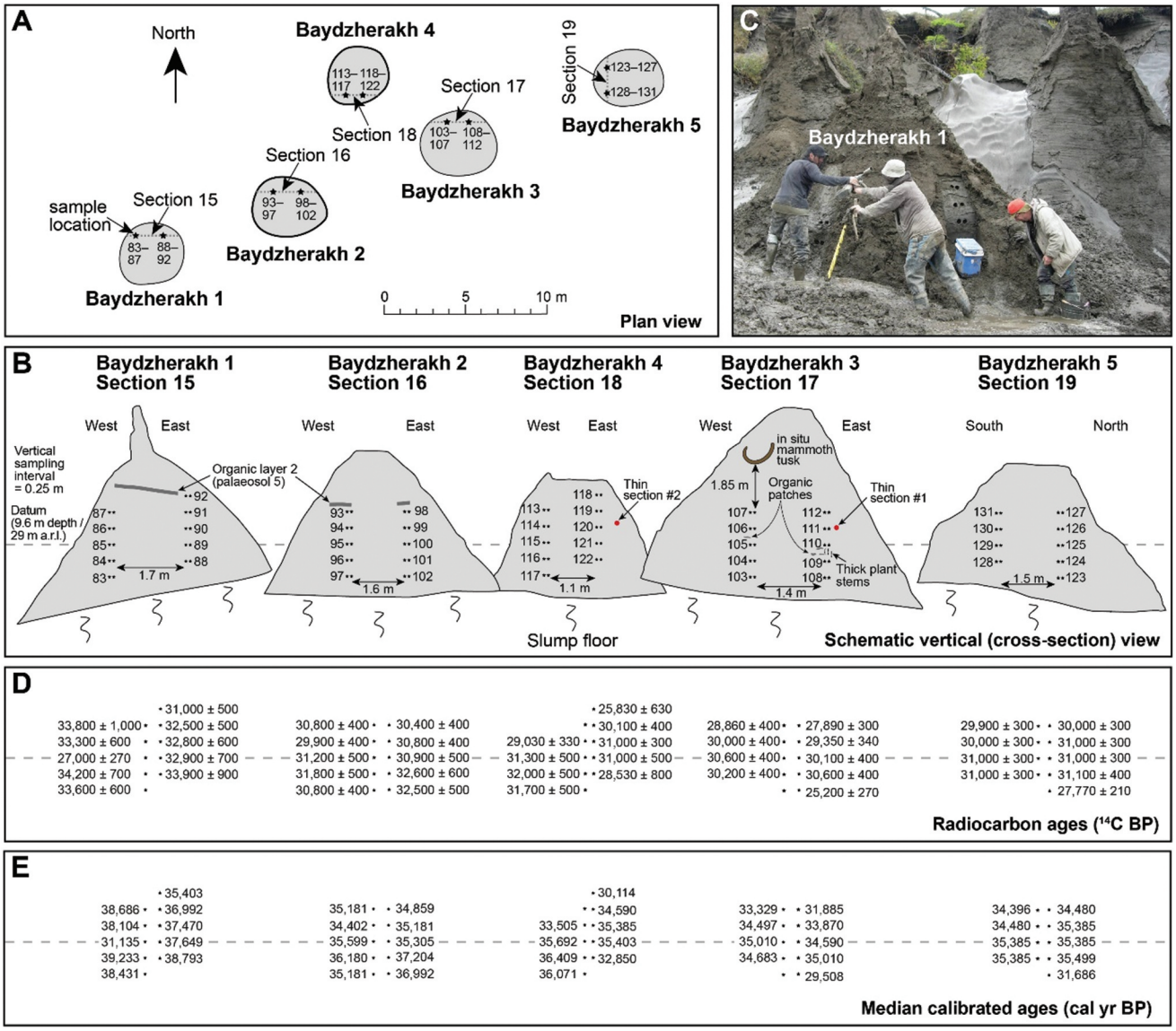

Figure 3. Location of the horizontal transect: (A), Plan view of horizontal spatial relations of the five baydzherakhs; (B), Vertical view of the detailed sampling scheme; (C), Photograph of sampling; (D), Original 14C ages; (E), Median calibrated ages.

University in Poznan. For more details, see Murton et al. (2015). We updated the original Bayesian age–depth models presented by Murton et al. (2015) using Oxcal v.4.4.4 and the IntCal20 radiocarbon calibration curve (Bronk Ramsey 2009; Reimer et al. 2020; see SI text 1 for further details).

The age-depth model for the 2009 composite vertical yedoma sequence follows the same stratigraphic order as outlined by Murton et al. (2015). Data from the individual sections (henceforth we use "S" to denote the individual sections) that fall within the range of radiocarbon calibration (S9, S10, S11, S12, and S13) were placed within P_Sequence models (Bronk Ramsey 2008) and nested within a sequence that included optically-stimulated luminescence (OSL) data from near the base of the exposure. This provided further constraint on the age-range of S8, which lies at or near the limit of radiocarbon calibration.

Laboratory analyses of sediments and pollen

Sedimentological analyses are detailed in Murton et al. (2015): sediment properties, magnetic susceptibility, geochemistry, and micromorphological examination of thin sections. A selection of samples across the height of the Duvanny Yar section was processed for pollen and counted at the North-East Interdisciplinary Science Research Institute, Magadan, using conventional approaches as described by Paleoclimate from Arctic Lakes and Estuaries (PALE; 1994) protocols. While pollen preservation in yedoma silt can often be good, some localities have poor preservation (M.E. Edwards, personal observation). In general, pollen retrieved from this Duvanny Yar locality was of poor quality and concentrations were low. Of countable samples, 12 came from the datable portion of the main section (Murton et al., 2015) and only three from the horizontal transect (from baydzherakhs 1, 2, and 3; this study). Counts are reported as percentages of the sum of terrestrial taxa (we included *Varia*, or unknown grains). Terrestrial spores were excluded from the sum and plotted as individual sums for the vertical transect as values varied widely. They were included in the main sum in the horizontal transect, as they occurred rarely.

Seda*DNA analyses*

Our focus for *sed*aDNA data is on vascular plants, bryophytes (both methods) and mammals (shotgun only). Samples came from the main section above 25 m arl (above river level; Figure S1) and the baydzherakh transect. For samples from the main section both methods were applied but only metabarcoding for the transect samples.

For the metabarcoding, *sed*aDNA samples were extracted using a PowerMax soil kit, following the protocols described by Yoccoz et al. (2012). The description below follows Willerslev at al. (2014), where further details can be found.

For the metabarcoding, PCR amplification used tagged (nine base pairs) generic plant primers for the P6 loop of the trnL plastid region ("g-h"; Taberlet et al. 2007). Each sample was amplified five times. Replication of the PCR process for each sample in metabarcoding reduces the uncertainty of false negatives and allows some estimation of rare vs. abundant taxa (Ficetola et al. 2015; Alsos et al. 2016). In this pioneering study, amplifications were variably successful, and the reads reported come from one to five replicates. In addition, samples were amplified once with primer pairs for the nuclear ITS1 region, which has the potential to differentiate taxa more effectively than the trnL region within some key groups (e.g., Poaceae, Asteraceae); this can also enhance overall read counts for these families.

Amplicons were sequenced using an Illumina GA IIx platform. Raw reads were processed using the Obitools software package (http://www.grenoble.prabi.fr/trac/OBITools) to provide a clean dataset. Sequences were compared against a specially constructed northern plant taxon database and the more cosmopolitan European Molecular Biology Laboratory (EMBL) database (see Willerslev et al. 2014). Matches to the database had to be ≥98 percent. *Salix* was excluded from the final dataset as it appeared as a contaminant in sequencing controls. Food plants and contaminant taxa identified via their appearance in processing blanks were eliminated. The recovered taxa were checked for biogeographic appropriateness and for possible conflation when two taxa have almost identical g–h sequences (see Willerslev et al. 2014 for further details). Some original metabarcoding MOTUs at the sub-genus level contained many species. These were checked to ensure biogeographically appropriate taxa were present; for analysis and clarity of representation, however, such taxa were merged into a higher taxonomic unit (e.g., genus; Table S1).

Shotgun analysis followed the methods described in Wang et al. (2021). DNA was extracted and purified following the InhibitEx protocol. Sequencing library preparation and quality controls followed the standard Illumina library preparation protocol (Meyer and Kircher 2010). Libraries were thereafter pooled and sequenced on an Illumina HiSeq 4000 platform. Sequencing data were first quality-controlled by trimming sequencing adapters and poly-X ends. PCR duplicates were then removed (for details of these steps, see

Supplementary text 2 [SI text 2]). Each quality-controlled read was given an equal chance to be aligned against all genomes in a comprehensive reference database using bowtie2 (version 2.3.2; Chen et al. 2018). The database comprised NCBI-RefSeq, NCBI-nt, PhyloNorway plant genome database, and an assembled Arctic fauna genome database (for further information about the reference database, see SI section 9.2.1 in Wang et al. 2021). We kept 1,000 hits (–k 1,000) for each read against each of the 53 database subdivisions of the reference database. We merged the 53 generated bam files per sample and sorted the merged bam file using SAMtools (Li et al. 2009).

For shotgun-based plant analysis, we first parsed only alignments with 100 percent similarity to reference data (see SI text 2 for more information). Taxa were then merged to the genus level; this required as a first step a threshold of five unique reads per taxon to remove noise. A series of filters and verifications were applied to authenticate identified plants. For each sample, we first removed the taxa represented by less than 1 percent of the total reads assigned to plant kingdom (Pedersen et al. 2016). A k-mer based approach for quantifying the effects of reference database availability for different taxa combined with authentications using read abundances was then applied to confirm the identified plant genus against a curated Arctic flora and fauna checklist (see SI text 2 and section 9.4 in Wang et al. 2021 for more details). For estimating the relative biomass abundance for plant taxa, we eliminated or normalized the identified read number per taxon against three variables: DNA damage degrees, sequencing depth among samples and read classification efficiency among taxa (see SI text 2 and section 9.5 in Wang et al. 2021 for more details). We authenticated the DNA damage patterns of identified plants for this study, going beyond the original 2021 analysis (See SI text 2).

For shotgun-based faunal analysis, reads classified at either family (when there is no unambiguous arctic genus under that family) or genus level were used for authentications. Alignments with a maximum of two mismatches were parsed. Only reads perfectly aligned to the faunal taxon's genome, and meanwhile not mapped to any other taxa across the comprehensive reference database (with one or two mismatches), were kept as reads to that given faunal taxon. At least five of these exclusively faunal reads in a sample were required for authenticating its identification in that sample. MapDamage (version 2.0.8; Jónsson et al. 2013) was used for estimating the DNA damage per faunal taxon per sample, and the average C to T and G to A mutation frequencies of the first position (F) and the mean of 4–25 positions (R) on identified fauna DNA strands were calculated. A minimum F/R rate at 2.0 was required for confirming the ancient origination of faunal DNA. More details can be found in SI section 9.6 in (Wang et al. 2021).

We applied a conservative approach for dealing with the potential contaminations and/or false positives identified in negative controls for DNA extraction and library preparation for shotgun analysis. First, given that fewer sequencing reads occur in controls, we reduced the read number threshold required for confirming a taxon from five to two to increase the sensitivity for contaminant detection. Next, we accounted for the index-hopping issue in single indexed libraries by comparing the proportion of a taxon's reads in the control dataset against the taxon's read proportion in the sediment sample sequenced in the same pool. This was followed by comparing the taxa identified in each control against i) the Arctic flora and fauna checklist and ii) the taxa identified in the sediment samples processed and sequenced in the same processing and sequencing batch. A greedy approach (i.e., fast, efficient, but with some level of imprecision) was then applied by merging taxa identified across all negative controls of the original 2021 study. This yielded a list consisting of 1,646 taxa as potential contaminants. All listed taxa were then subtracted from the taxonomic profile of each sample. More details can be found in the SI section 9.3 in (Wang et al. 2021).

Data analysis

We explored the data using all molecular taxa, noting MOTUs of any taxonomic level that provided ecological information. We compared the taxon lists generated by the two approaches to check for ecological consistency and degree of overlap. After checking, we merged the two datasets at the genus level (exceptions being subfamily and family for Poaceae; tribe and family for Asteraceae); this retained a high level of ecological information and afforded easy comparison. Merged datasets were used to display results for the late-Pleistocene and Holocene samples from the main section.

The metabarcoding data lack the number of PCR repeats expected today, and the taxon assignments use an older reference database. We thus reviewed the data in relation to overall reliability, the meaning of read numbers and data presentation using presence-absence vs abundance. To present and analyze the data further, we tried square-root normalizing read numbers and converting to percent, but originally high read numbers still distorted percentage values. We therefore converted the data to a categorical log scale (0, 2, 4, 6, 8, where 0 = <10 reads and 8 = >10,000 reads). This facilitated

plotting and made the categories of read abundance visually accessible, providing a "believability" estimate of both presence and likely abundance in the local biomass for each taxon in each sample.

Visual representation of plant and mammal MOTU frequency through time, and of MOTUs and pollen taxa from the transect of baydzherakhs was done using the program TILIA (Grimm 1992; available at https://www.neotomadb.org/apps/tilia).

For the horizontal transect only (38 samples, metabarcoding), we assessed patterns of variation among *sed*aDNA samples based on MOTU composition via multivariate analyses. A few taxa were common/abundant and had high values, while other taxa occurred only once or a few times. Both principal components analysis (PCA) and detrended correspondence analysis (DCA) proved sensitive to the inclusion or omission of these rare taxa and to the use of percentage vs categorical data. A good spread of samples with the fewest taxa omitted was found with a PCA using the categorical dataset (40 taxa) and a DCA with percentage values (38 taxa). Ordinations were computed using PAST v 4.03 (Hammer, Harper, and Ryan 2001).

We did not apply rarefaction to the dataset, as it is not relevant to qualitative (ecological) properties or ordination. We tested for correlation between sample scores from ordination axes 1 and 2 between a) height in section and b) radiocarbon age, which are similar, but not identical, variables.

Results

Chronology

The chronology established for the 2009 sampling locality is the most comprehensive so far from Duvanny Yar. The main section chronology was originally reported – and compared with other chronologies – in Murton et al. (2015). Calibration with IntCal20 and the nesting of *P_Sequence* models and OSL dates within a wider *Sequence* model alters it slightly. Samples higher than ca. 25 m arl have finite dates and form a coherent upward sequence (Figure 4A). We took a cautious approach to dates, as radiocarbon ages >ca. 30,000 ^{14}C yr BP can be uncertain due to the rapidly decaying count-rate. The most prominent change occurs in S8, which results in younger dates when informed by the underlying OSL dates. Nevertheless, S8 yielded dates >40,000 ^{14}C yr BP and its age may not be finite; it underlies a paleosol and hiatus (Figure S1) and was therefore excluded from our analyses.

Radiocarbon dates, plus one OSL date (Shfd 10105), for S12, S13, and S14, show good continuity through the period ca. 30,000 to 20,000 cal. yr BP. They thus fall broadly within MIS 2. Samples in S9, S 10 and S11 are also stratigraphically consistent, with ages between ca. 38,500 and 35,000 cal. yr BP, and they lie within MIS 3. A prominent temporal discontinuity at ca. 31 m arl aligns with a discontinuous paleosol but also with a sampling shift to a different vertical section (Figure 4A).

In terms of the stratigraphic framework used in the Russian literature, four samples from S12 and S13 are <25,000 and >15,000 cal. yr BP, thus falling within the regionally identified Sartan late-glacial maximum. The older MIS-2 samples and those in S9, S10, and S11 (MIS 3) are assigned to the Karginsk Interstadial (55,000–25,000 cal yr BP; Murton et al., 2015; Anderson and Lozhkin 2001). Here we use the global terms MIS 2 and 3 (see above) to allow for a wider geographic comparison of results. The sampled baydzherakh material (sections S15–S19) lies in the age range ca. 39,000–33,000 cal. yr BP, but baydzherakh 1 (B1) is older than the other four (Figure 3). The baydzherakh transect is dated by 47 radiocarbon samples. Full information on original radiocarbon dates and 2-sigma age ranges for calibrated ages (Figure 4B) is given in Table S2.

Sediment properties and stratigraphy

The materials sampled in the main section and in the baydzherakhs fall within Unit 4 of Murton et al. (2015) and are described as yedoma silt. The sediment is texturally homogeneous and generally unstratified. It displays subtle color banding when freshly exposed, which relates to the nature and abundance of organic remains. The banding disappears on exposure to air, and the sampling scheme did not capture it. Further details of geochemistry and microstructure are available in Murton et al. (2015). In the baydzherakh transect, the location of a thin, gently dipping paleosol (Paleosol 5 of Murton et al., 2015) in relation to other samples is shown in Figure 3. Four sets of samples with the same or similar ages plotted against height indicate a shallow syncline and an apparent dip north-eastwards from B1 toward B3, suggesting locally variable sedimentation rates and an undulating paleo land surface (Figure 5).

Pollen data

The pollen samples DY92, DY100, and DY110 come from baydzherakhs 1, 2 and 3, respectively (B1, B2, B3; Figure 3; Table S3). A total of 26 pollen and spore types are identified in the three samples; pollen sums range from 158 to 247. DY92 and 100 are dominated by Poaceae pollen (50–60 percent), and DY110 is

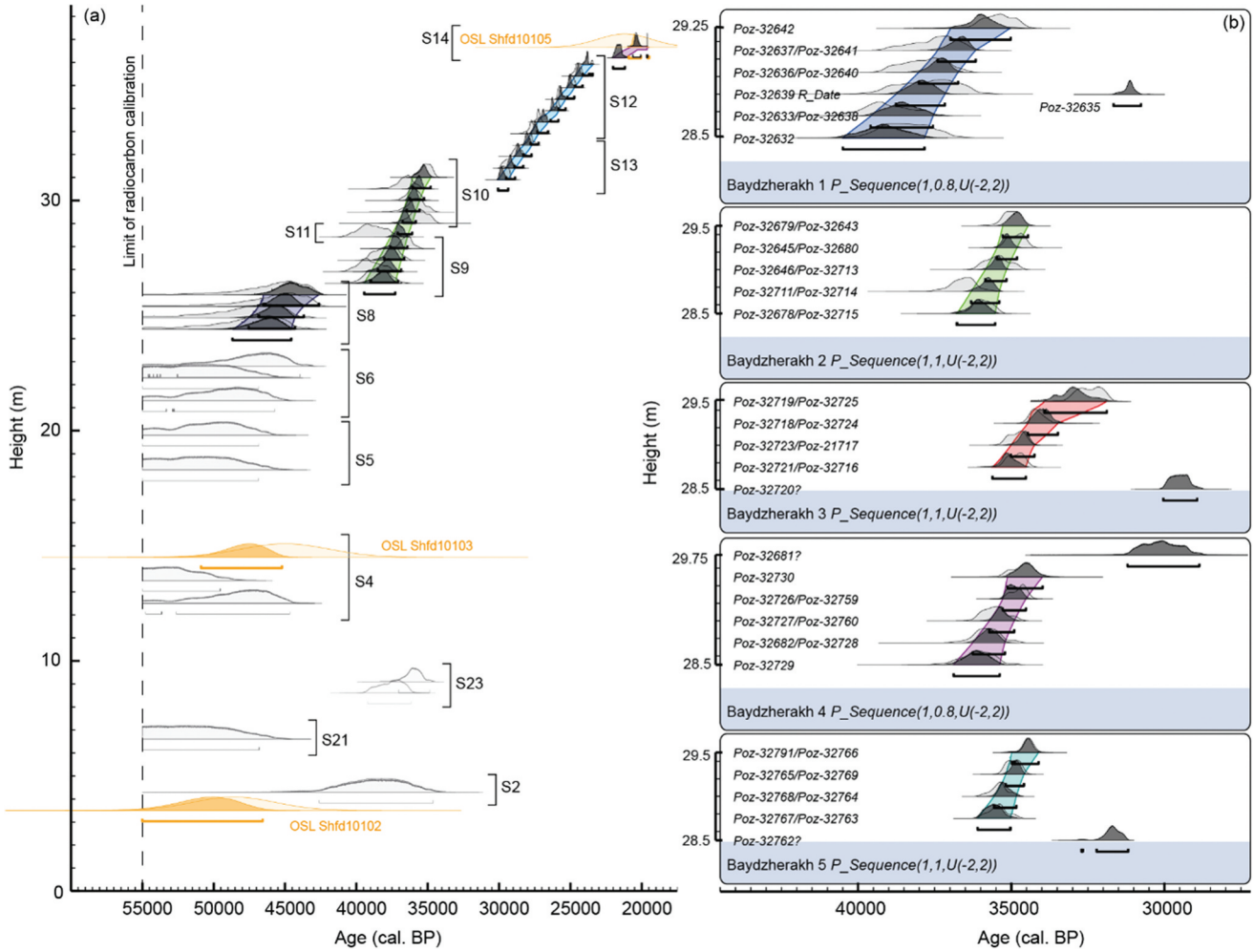

Figure 4. (A) The OxCal age–depth model for Duvanny Yar main section. Radiocarbon dates from section 8 are likely non-finite; pale gray dates from below section S8 indicate other dates that produced a finite age but are not considered reliable. Non-finite dates are not shown. (B) OxCal age–depth models for the baydzherakh sections.

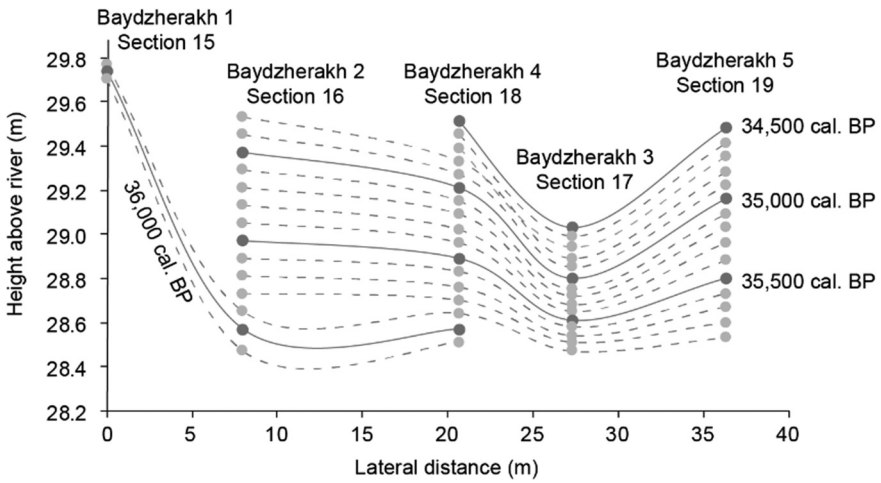

Figure 5. Heights for four coeval surfaces across the horizontal Baydzherakh transect inferred from the independent OxCal age-depth models.

dominated by Caryophyllaceae. All samples contain Asteraceae pollen (includes Asteroideae and Cichoridae), but with values of 5% or less, and *Artemisia* is uncommon. Other forb families and genera include Brassicaceae, *Papaver*, Ranunculaceae, and Saxifragaceae. Modern regional tree and shrub taxa (*Larix, Betula, Salix, Pinus, Alnus*, and Ericales) are present but at 5% or less. The non-vascular plant *Selaginella rupestris* occurs at 5 percent or less (Figure 6).

The pollen and spore taxa for the baydzherakh samples and samples from the same period in the main section (published in Murton et al., 2015; Figure S2) are similar; other taxa recorded in the main section are *Salix*, Valerianaceae, Primulaceae, Onagraceae, Gentianaceae, and Polypodiales.

Seda*DNA*

In the original metabarcoding analysis of Willerslev et al. (2014), some samples failed, and others had very few sequencing reads. The total number of reads for samples dated <40,000 cal. yr BP was ca. 2.4 million. Twenty-two original metabarcoding samples from the main section had usable data and finite dates <40,000 cal yr BP, including five from the latest Holocene (see Figure S1; Table S4). Of an original 44 samples collected from the horizontal transect, 38 were usable. The 101 MOTUs derived from the metabarcoding dataset for the horizontal transect (prior to merging) comprise about 1.6 million reads. The MOTUs were merged to higher taxonomic levels for clarity, and the 38 resultant taxa were used for multivariate analysis (Table S4).

Of the 40 samples analyzed by shotgun sequencing, one sample failed to generate sufficient reads. A total of ~1.16 billion raw sequencing reads was generated for the remaining 39 samples, with ~1.03 billion reads (average read length ca. 69) passing the quality controls and thus used for taxonomic profiling. Finally, ca. 70.10 million reads were classified to a plant or animal taxon under the genus level. Of the thirty-nine samples, twenty-eight had finite ages; these were used for this analysis. Shotgun-identified taxa merged to genus and full details of original reads and normalized reads are given in Table S4 (plants) and Table S5 (vertebrates).

Analysis of sequence ends shows increasing damage in the first ca. six read positions, based on read lengths of 30–80 (Figure 7), confirming the conclusions of Wang et al. (2021) that the *sed*DNA is ancient.

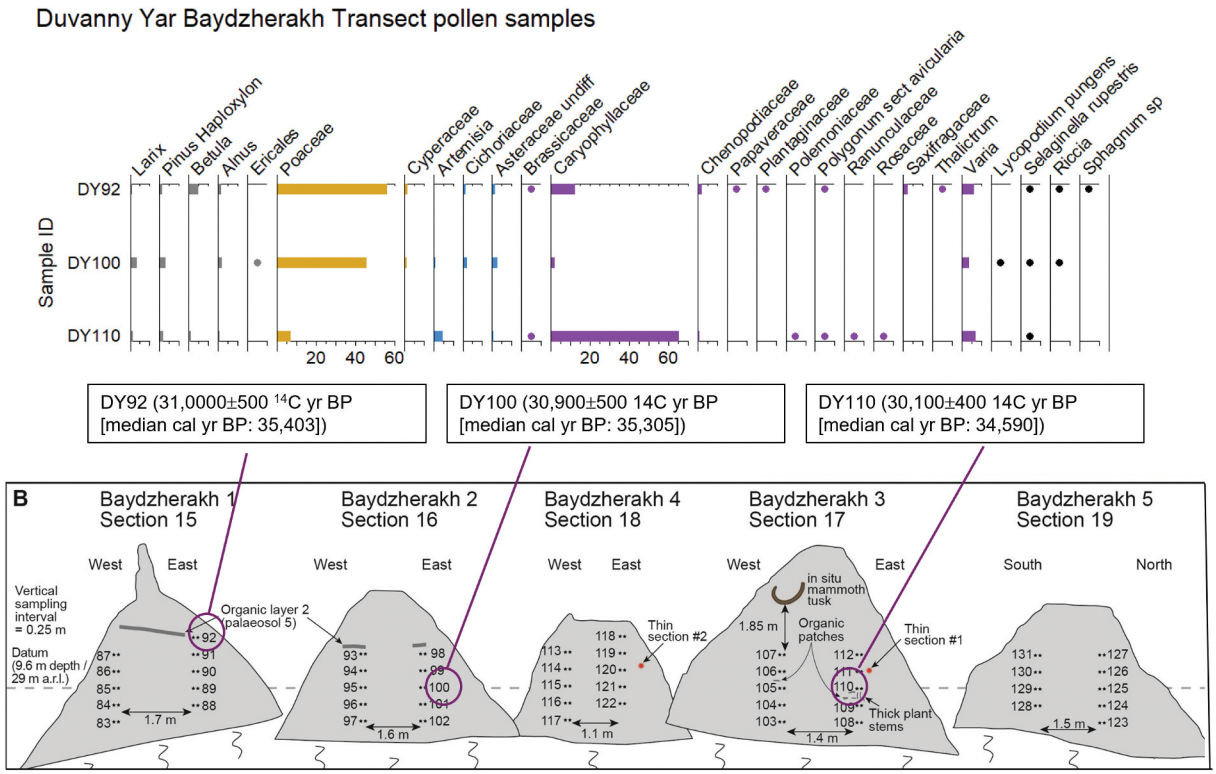

Figure 6. (A). Pollen and spore data for horizontal transect shown as percent total sum. Functional groups are color coded, L to R: woody taxa (gray), graminoids (gold), Asteraceae (blue), other forbs (magenta) and spore-bearing plants (black). Pollen and spore sums: DY92 (233); DY100 (158); DY110 (247). Sample locations and ages are shown below the pollen diagram.

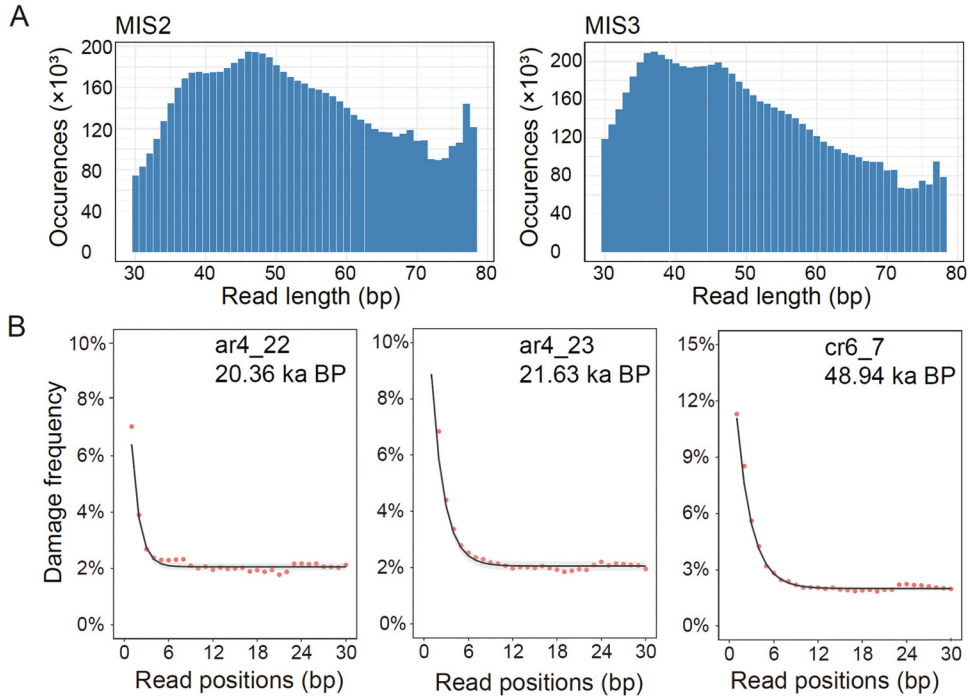

Figure 7. Ancient DNA damage patterns for identified plant DNA reads. (A) Read number of all authenticated plant reads across samples from MIS2 and MIS3 plotted against read length. (B) Postmortem deamination DNA damage modeled at node Viridiplantae (covering all reads assigned to this node and below) for three samples. X-axis indicates the first 30 read positions from the 5′ end. Red dots indicate the frequency of C to T substitutions at each position modeled by metaDMG. The solid line was generated by binomial regression, with the pale gray area representing 95 percent confidence interval.

Main section

The metabarcoding and shotgun plant datasets show considerable overlap at genus level (filtered samples only; Table 1): 50 percent shared; 22 percent metabarcoding only; 28 percent shotgun only.

More importantly, all the taxa identified in the two datasets make paleoecological sense for the intervals in question, and together they enhance floristic richness.

Table 1. Comparison of *sed*aDNA plant genera: metabarcoding and shotgun metagenomic datasets for paired samples from the main transect, Duvanny Yar, plus metabarcoding taxa added from the horizontal transect (in parentheses).

Metabarcoding only (10)	Shared genera (23)	Shared genera	Shotgun only (13)
Empetrum	*Arctagrostis*	*(Galium)*	*Alopecurus*
Eritrichium	*(Anemone)*	*Oxytropis*	*Astragalus*
Gaylussacia	*Artemisa*	*Papaver*	*Bistorta*
Juniperus	*Betula*	*Plantago*	*Calamagrostis*
Koeleria	*Bromus*	*Poa*	*Dactylis*
Leymus	*Carex*	*Potentilla*	*Dryas*
Primula	*(Cerastium)*	*Puccinellia*	*Epilobium*
Senecio	*Elymus*	*Ranunculus*	*Equisetum*
Tanacetum	*Eremogone*	*Tephroseris*	*Eriophorum*
(Hordeum)	*Erigeron*	*Trisetum*	*Larix*
	Festuca	*Vaccinium*	*Oreojuncus*
	Myosotis		*Pedicularis*
			Salix

In the vertical transect, three distinct units are defined by sampling hiatuses that are consistent with the latter part of MIS 3, MIS 2, and the latest Holocene (Figure 8).

Horizontal transect

For the transect metabarcoding taxa, the categorical read-abundance values are ordered into broad functional groups (Figure 9). Taxa are evaluated on frequency (the number of samples in which they occur) and abundance (read number category, with 3–4 being abundant). The only woody taxon is *Empetrum*. Grasses are frequent; the subfamily Pooideae includes all taxa higher than genus level. Of the seven identified grass genera, *Festuca* is the most frequent and abundant. Sedges are only occasional, however. Anthemidae, a genus-rich tribe of the Asteraceae that includes *Artemisia*, is also abundant in most samples, and *Tanacetum* is abundant where it occurs. Several other forbs (e.g., *Myosotis alpestris*) tend to occur with high abundance but less consistently. Other forb taxa tend to be infrequent, except for *Plantago canescens*, which is frequent and abundant. The moss family Polytrichaceae is abundant where it occurs. *Myosotis* and *Potentilla* are somewhat clustered in B3, but

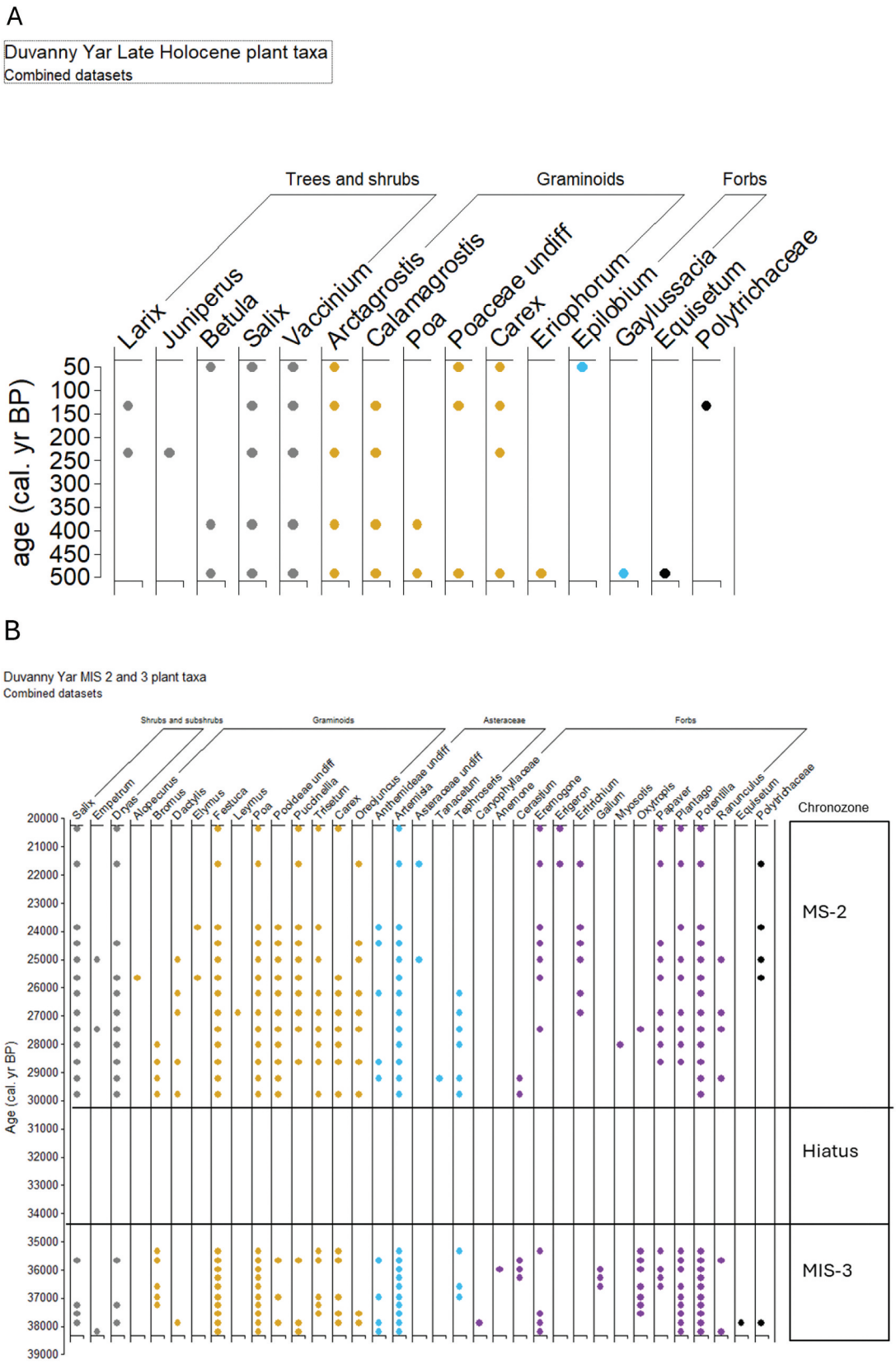

Figure 8. Merged plant *sed*aDNA record, main section, Duvanny Yar (A). Late Holocene. *Larix*, *Juniperus*, *Betula*, *Vaccinium*, *Arctagrostis*, *Calamagrostis*, *Epilobium* and *Galussacia* only occur in the late-Holocene samples. (B). MIS 3 and MIS 2 samples.

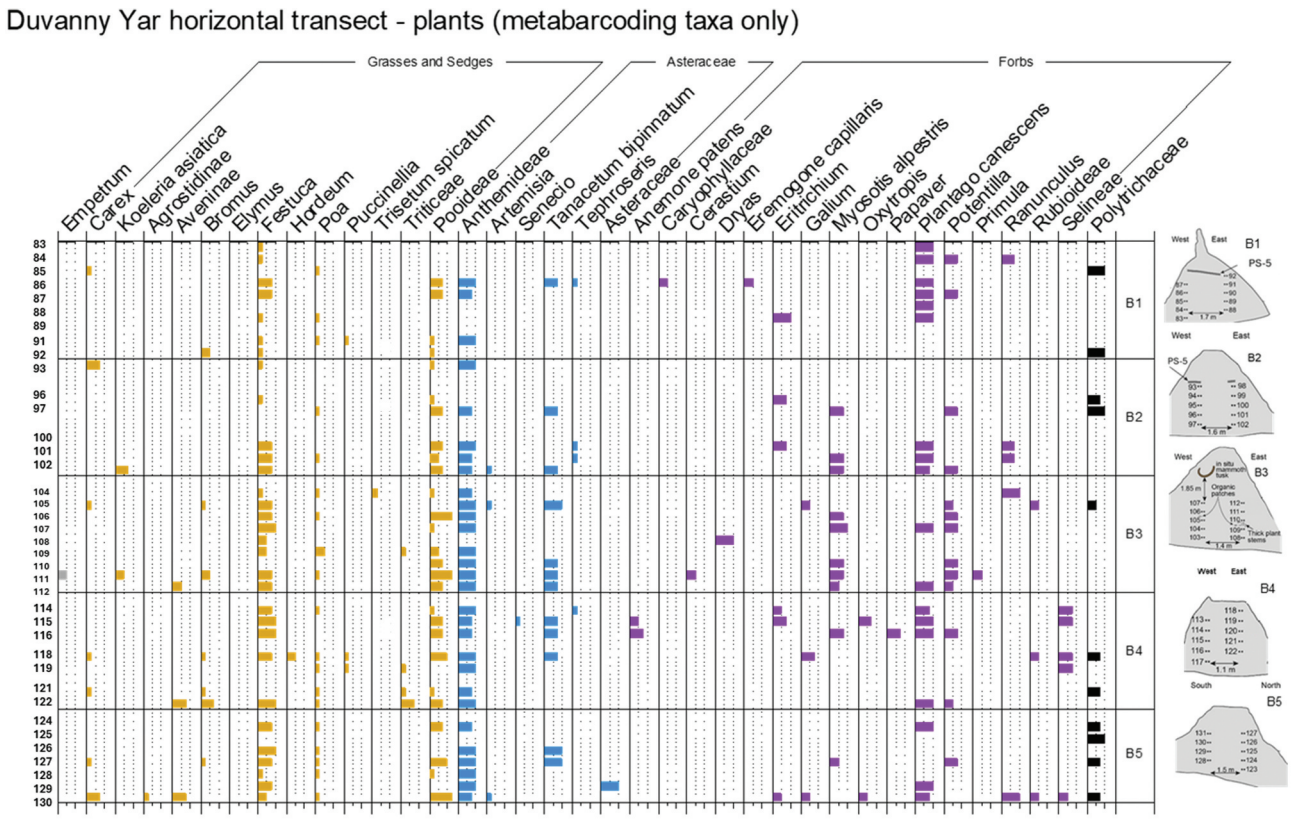

Figure 9. Horizontal Transect. Metabarcoding *sed*aDNA merged MOTU values log normalized (X-axis values: 1 ≥ 10; 2 ≥100; 3 ≥1000; 4 ≥10,000). Forbs include all taxa outside Asteraceae. Zone lines separate the five baydzherakhs. Baydzherakh mini-profiles locate each sample (see Figure 3 for radiocarbon ages). Vertical axis: sample number.

otherwise, there are no clear patterns associated with the individual baydzherakhs.

The first three axes of the PCA on the categorical dataset account for 24.13 percent, 17.45 percent and 11.10 percent of the variance, respectively, leaving just under 50 percent of the variance unexplained. Taxa have generally low loadings on the first three axes. Figure 10 shows a scatter of samples with little spatial pattern. The DCA on percent values (Figure S3) shows a similar lack of pattern but high turnover among samples (lengths of axes 1 and 2 were both ca. 4.0 standard deviations, suggesting complete turnover of samples on axes). Eigenvalues were high: 0.663 and 0.353, respectively (but note this does not precisely reflect variation explained). There was no significant correlation of any ordination scores with age or position of samples (R^2 values <0.1).

The mammalian sedaDNA record

The shotgun data include six taxa (Figure 11, Table S4). The most frequent are horse (*Equus* spp.) and hare (*Lepus* spp.). Woolly rhinoceros (*Coelodonta antiquitatis*), steppe-bison (*Bison priscus*), and reindeer (*Rangifer tarandus*) are only recorded in MIS 2. Vole (*Microtus*) is also sporadically present. The presence-absence data are plotted (Figure 11) with published dated fossil-bone data from Sher et al. (2005), Andreev et al. (2009), Kuznetsova et al. (2022), and Fordman et al. (2024).

Discussion

Stratigraphic and temporal accuracy of Duvanny Yar data

The chronology from this Duvanny Yar study is the best obtained to date for the site. The overall temporal profile from S9 upward in the main section, and the largely vertical coherence within each of the five baydzherakh sections (i.e., few reversals) suggest that there is little redeposition or modern contamination of the samples. The damage patterns from shotgun data indicate the DNA is ancient, not modern contamination (Figure 7). The approximate average sediment (and contained ice) accumulation rate for the sections <40,000 ^{14}C years old is ca. 1–2 mm per year, based on the radiocarbon chronologies of the main section and the baydzherakhs.

There is a degree of uncertainty, however, as to where any given sample lies in time when compared spatially

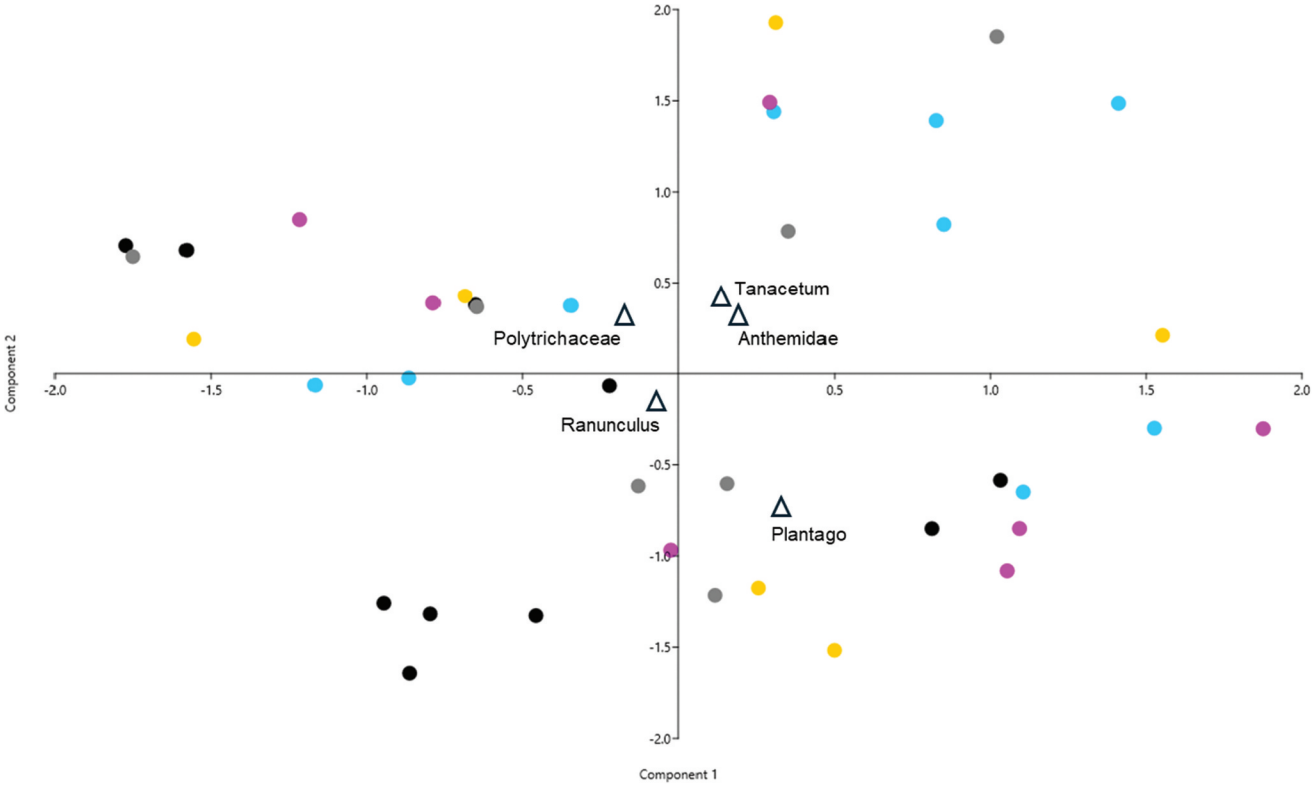

Figure 10. PCA biplot of samples and taxa on axes 1 and 2 (scaled as eigenvalues). Baydzherakhs 1–5 are color-coded (B1-black; B2-gold; B3-azure; B4-fuschia; B5-gray). Taxa with highest loadings on axes 1 and 2 shown in each quadrant.

with neighboring samples, partly due to dating error, but also because of small variations in rates of upward accumulation, as shown by the syncline across the transect and an implied dip north-eastward from B1, which has an older basal date than the other baydzherakhs (Figures 4 and 5). Furthermore, a depositional hiatus is evident in the main section at ca. 30–31 m arl (between S10 and S13; Figure 4, Figure S1) at the level of a discontinuous paleosol. The B1 paleosol at ca. 29.75–30.0 m arl dates from ca. 32,000–31,000 14C yr BP (ca. 37,000–35,000 cal yr BP) and is likely the same horizon. Murton et al. (2015) interpreted the discontinuity as a cessation of silt deposition over about 4,000 yr from about 35,000 cal yr BP, which is consistent with paleosol formation, either broadly across the landscape or locally, perhaps due to undulating paleo-relief. Zanina et al. (2011; see below) described a paleosol of similar age at other Duvanny Yar localities.

Bioturbation or downward penetration of roots from younger surfaces (or of other material via root channels) as the yedoma silt accumulated could alter the *sed*aDNA composition prior to freezing within the upward aggrading permafrost. This would be perhaps 300–800 yr after deposition, and assuming the palaeo-active-layer thickness was approximately 60–80 cm (inferred from the depth of the base of the store chambers of infilled rodent burrows relative to the palaeo-land surface at Duvanny Yar; Zanina 2005) and the sediment accumulation rate of ca. 1–2 mm per year, as discussed above. A paleo-active layer thicker than the present active layer is likely to have developed because during accumulation of yedoma silt an insulating surface organic layer was almost certainly thinner, or absent, compared with the present organic layer (Murton et al., 2015; Shur 1988; Guthrie 2001). Murton et al. (2015) reported relatively little incorporation of modern material (such as roots) in the uppermost portion of Duvanny Yar prior to freezing, but, more generally, root penetration does occur in unfrozen sediments and its consequences should be investigated further (see Clarke et al. 2021; Lupachev et al. 2025). Nothing in the dataset indicates this kind of contamination, however.

Comparison of plant sedaDNA *and pollen*

The most striking aspect of the three floras is not their moderate degree of taxonomic overlap (Table 1); rather, the joint flora forms a consistent whole that indicates the same ecological conditions. *Sed*aDNA and pollen data partly overlap and are partly complementary; these

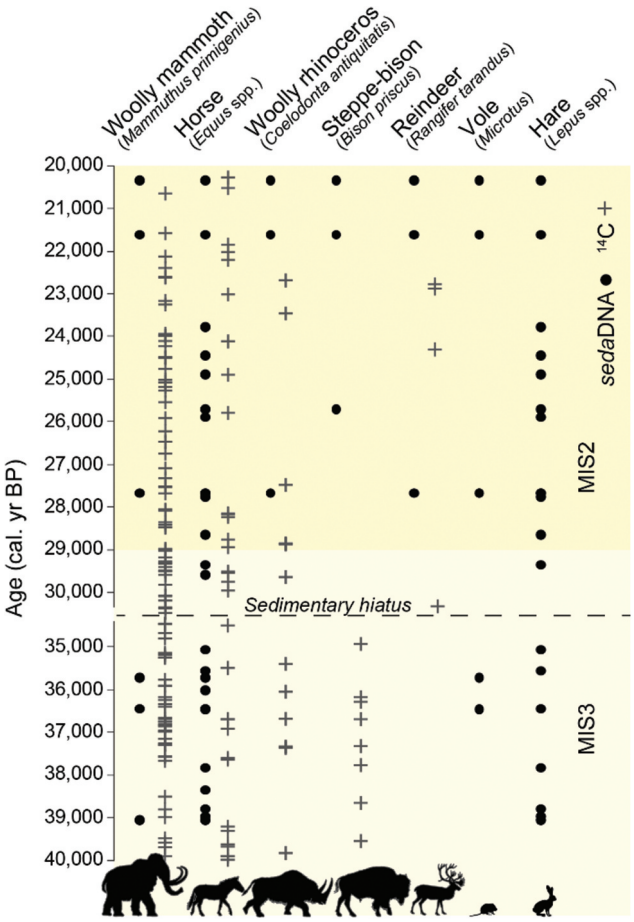

Figure 11. Mammalian *sed*aDNA records from Duvanny Yar main section (presence-absence, filled circles) compared with regional radiocarbon-dated fossil records (+; Sher et al. 2005; Andreev et al. 2009; Kuznetsova et al. 2022; Fordman et al. 2024). NB Lepus and Rodentia are listed but not dated.

proxies sample different landscape spaces (Jorgenson et al., 2012; Parducci et al. 2019; Monteath et al. 2023). The Duvanny Yar pollen includes a range of tree and shrub taxa (*Pinus, Larix, Betula, Alnus*), albeit at low levels (Figures 6, S2). The woody pollen types were probably transported over a distance from moister locations within the region, such as river valleys. The widely dispersed *Pinus* pollen may have traveled a considerable distance, possibly from beyond the lower Kolyma region. It is also conceivable that some grains are retransported and/or reworked locally by wind, given the prevailing conditions were favorable for loess deposition (see Andreev et al. 2011). *Pinus* and *Alnus* are absent from the shotgun dataset, and *Larix* and *Betula* occur only in Holocene shotgun samples.

From a comparison of the metabarcoding and shotgun datasets, several important differences emerge. First, although *Salix* is represented sporadically in MIS 3 and 2 in the shotgun data (it was present but excluded from the metabarcoding data—see above), it comprises 12 percent of the total reads, suggesting it was almost certainly present. Second, while species in the Asteraceae were undoubtedly important in the paleoflora, it is likely that ITS bias in metabarcoding over-emphasizes their importance, as suggested by the far higher proportional contribution of reads to the metabarcoding dataset (40 percent metabarcoding vs 17.3 percent shotgun). Total forbs values are also elevated in the metabarcoding data (79.5 percent metabarcoding vs 45.1 percent shotgun). Finally, the molecular data also show high values of *Artemisia* and the Anthemidae tribe of Asteraceae, which includes *Artemisia*, but *Artemisia* has low values in the pollen data, perhaps suggesting that the molecular Anthemidae group represents the presence of as-yet unidentified floristic diversity in these ancient communities.

Representation of the local paleoflora by sedaDNA

In modern tundra soils, metabarcoding *sed*aDNA records overlying, above-ground plant taxa, though not completely (Yoccoz et al. 2012; Edwards et al. 2018). Whether such a relationship holds for soils more broadly across vegetation types and time is a key question. Yedoma silt at Duvanny Yar is ancient incipient soil ("cryopedolith"), albeit poorly developed due to rapid burial and syngenetic freezing (Gubin 2002, cited in Murton et al., 2015; Lupachev et al. 2025). Given previous results, we assume that many taxa from the associated vegetation will be absent from any one sample, but multiple samples may identify a fuller complement of taxa, parts of a small-scale mosaic or even different plant communities. Indeed, per-sample metabarcoding MOTU numbers are relatively low for the transect: a mean of 13.4 for all identified MOTUs, but 7.4 for the reduced taxon set that merged nested MOTUs. For the metabarcoding and shotgun datasets based on genera the means are 7.5 and 9.5, respectively.

In both datasets, taxon richness per sample varies considerably, which underlines the uncertainty in placing emphasis on any one sample in an interpretation. Some samples show "spikes" in one or more taxa, which may relate to PCR bias. It may also be the case that the amount of soil material sampled is just too small; the *sed*aDNA will not be as well mixed as it would be in, for example, water or lacustrine sediment. For the time slice 35,000–30,000 cal. yr BP, adding new taxa cumulatively from 12 samples to reach a total of 23 taxa typically needs all 12 samples to reach the full observed taxon pool. At Duvanny Yar, sediment characteristics, as well as small sample volume, may also contribute. Pollen preservation at Duvanny Yar is rather poor, which may indicate generally low preservation potential of organic

material. We conclude that floristic diversity from yedoma samples can be enhanced by using joint MB–MS datasets and a higher number of metabarcoding PCR repeats (i.e., 8–12; Ficetola et al. 2015; Alsos et al. 2016), and, possibly, starting with a larger volume of (mixed) sediment for each sample (e.g., Taberlet et al. 2012). New methodological approaches to *sed*aDNA analysis are also promising. For example, Murchie et al. (2021b) retrieved more taxa per sample from Yukon loess samples using a DNA-bait approach than were found in this study.

MIS 3 and 2

A rich suite of forbs characterizes all three MIS 3 and 2 datasets (Figures 6, 8B, 9 and S2). There is likely more convergence on source area of pollen and sed*a*DNA for forbs, as pollen of entomophilous forb taxa tends to be local in origin, so we may assume most taxa were growing near the sampling sites (exceptions are grasses and *Artemisia*, which produce abundant, widely dispersed pollen, and which could have local or distant sources). These taxa, along with the speciose family Caryophyllaceae, dominate the pollen spectra (aboreal pollen is unlikely to be locally derived, see above). The full-glacial pollen spectra from Bol'shoy Lyakhovsky Island to the northwest (Wetterich et al. 2011) are not dissimilar, being dominated by grasses, *Artemisia*, and pioneer tundra taxa (i.e., Caryophyllaceae, Brassicaceae, and Papaveraceae); they are interpreted as a species-poor tundra-steppe with lower biomass than bracketing warmer intervals. Similarly, arboreal pollen types are considered to be derived from long-distance transport.

Salix (willow) occurs in the MIS 2 and 3 molecular and pollen floras. Prostrate *Salix* is an abundant macrofossil in MIS 2 at Bykovsky Peninsula, central Siberian coast (Sher et al. 2005), as it is in a 21,000-year-old flora from yedoma on Seward Peninsula, Alaska (Goetcheus and Birks, 2001). It is a strong indicator of tundra today, and it underlines that modern zonal steppe (in which it does not typically occur) is not an exact analogue of the Pleistocene cold-stage vegetation. Other taxa are more ecologically ambiguous. Grasses, such as *Festuca* and *Poa*, occur widely in both tundra and steppe. The forb genera, especially if speciose, range across different habitats. Some are typically associated with a range of tundra environments (e.g., *Myosotis alpestris, Papaver, Eritrichium, Oxytropis, Potentilla*, Brassicaceae) but may contain species that can also occur in boreal steppe, e.g., *Anemone patens, Plantago canescens*. Furthermore, several taxa contain species associated in the region today with disturbance, such as on steep and/or eroding slopes with loose sediments, and as colonizers of disturbed ground, e.g., *Bromus pumpellianus, Tanacetum bipinnatum*, Chenopodiaceae, and *Tephroseris*; the last (mastodon weed) is common on the yedoma exposures today as a successional species (Laschinskiy, Faguet, and Biasi 2020). Non-vascular plants are represented by several taxa in the pollen, most notably *Selaginella rupestris*, which is a typical component of late-Quaternary floras in western Beringia (Anderson and Lozhkin 2001). The bryophyte family Polytrichaceae is strongly represented in the metabarcoding *sed*aDNA. It comprises a large group of acrocarpous mosses, their growth-form likely to make them resilient during loess deposition. *Polytrichum juniperinum* is associated with "sedge heath" under cold, dry conditions in western Beringia today (D.I. Berman, personal communication, 1992; Sher et al. 2005 and references therein) and indicated in MIS 2 at other sites via the fossil occurrence of an obligate associate, the beetle *Morychus viridis* (Alfimov, Berman, and Sher 2003, cited by Sher et al. 2005; Sher and Kuzmina 2007).

The identities of many taxa point to the classic concept of steppe–tundra, that is, a vegetation containing taxa linked with modern steppe, those linked with tundra, and those that are found in both vegetation types today. There is a strong signal of dry, cold, and probably disturbed conditions, which aligns with regional loess deposition in MIS 3 and 2. The lack of widespread modern floristic analogues for these conditions or the observed paleovegetation (see above) may reflect the fact that consistent, if not continuous, loess deposition, which was fundamental to the creation of past yedoma landscapes, is highly restricted today. For example, Laxton, Burn, and Smith (1996) described a loess fertilization effect for contemporary vegetation receiving floodplain-derived loess input. For soil beneath the loess plume, levels of nitrogen and carbon were elevated, and vegetation biomass and species diversity were positively correlated with soil silt content. However, unlike the ice-proximal location of the Kluane Lake loess grassland described by Laxton, Burn, and Smith (1996), Late Pleistocene Duvanny Yar is thought to have been distant from glacial sediment sources. This topic deserves further attention; if the loess itself exerted physical control over steppe–tundra soil and vegetation productivity, temporal changes in loess input may explain subtle variations observed in the loess stratigraphy (see above) and, more broadly, levels of herbivore carrying capacity.

The late Holocene

As would be expected, the late-Holocene molecular flora is markedly different from that of MIS 3–2 and

consistent with a moist environment (Figure 8A). The identified molecular taxa occur today in the area and include *Larix* (the dominant tree species), and *Betula* and *Salix* (dominant shrubs). *Vaccinium* is a widespread dwarf shrub, and *Juniperus* occurs on dry sites. Of these taxa, only *Salix* occurs in MIS 2 and 3 samples in the shotgun dataset (see below). *Epilobium* (*Chamaenerion*) and *Gaylussacia* are largely boreal taxa, although the former also occurs in tundra.

The mammalian record

The Duvanny Yar *sed*aDNA records the presence of the well known late Pleistocene megafauna as well as smaller mammals (Figure 10). Horse is present throughout the record while woolly mammoth occurs in both MIS3 and MIS2 but is detected less frequently. Woolly rhino, steppe-bison and reindeer are only detected sporadically in MIS2 samples. Identification of smaller, burrowing mammals in the *sed*aDNA provides important evidence for the presence of these taxa, which are often poorly represented in the fossil record. The frequency of hare is high; the species is not defined, but we speculate that it is probably arctic hare (*Lepus timidus*), which occurs across northern Siberia today.

The *sed*aDNA record invites comparison with regional radiocarbon-dated fossil bone records (Sher et al. 2005; Andreev et al. 2009; Kuznetsova et al. 2022; Fordman et al. 2024). *Sed*aDNA and radiocarbon data for horse, woolly mammoth and reindeer are broadly consistent, although radiocarbon data are biased toward mammoth—likely because of collection bias. There are, however, interesting differences in data for woolly rhino and steppe bison. Fossils from both taxa have been radiocarbon-dated to between 40,000–35,000 cal yr BP, but their DNA is absent from the Duvanny Yar record during this period. While there are few radiocarbon-dated woolly rhino fossils from the Sakha Republic, steppe bison are well represented, and their absence from the MIS3 *sed*aDNA record is curious. Conversely, steppe bison are detected in several *sed*aDNA samples between 30,000–20,000 cal yr BP but are virtually absent from the regional fossil record. These data may represent "ghost ranges," where taxa are revealed by DNA while invisible to the fossil record (Murchie et al. 2021a), or, possibly, contamination following thermokarst (Arnold et al. 2011; Seeber et al. 2024), though we consider this unlikely. Further details of read numbers from other sites, particularly if mammal reads were more abundant than at Duvanny Yar, may provide a useful counterbalance to bone databases in an assessment of relative animal numbers and biomass and provide insight into the population dynamics of the Pleistocene herbivore guild.

Floristic variation across the MIS-3 landscape

Whether local variation in vegetation composition occurred across the Duvanny Yar transect, for example, as a response to local topography, is unclear. The PCA and DCA explain moderate to high proportions of sample variation (Figures 10, S3), depending upon small changes in the dataset used (e.g., omission of taxa with one or a few occurrences only). This variation, however, is not a temporal pattern, nor does it appear as a spatial pattern over ca. 10 m between sampling stations (i.e., baydzherakhs). Likely methodological limitations are that samples probably under-represent the local flora (Edwards et al. 2018; see above) and that the transect length of ca. 40–50 m is too short to identify taxon mosaics occurring on a scale of tens of meters. Based on the topography of the modern landscape and available stratigraphic information, it is likely that the paleo land surfaces of MIS 2 and 3 were gently undulating at most, thus reducing the chances of community differentiation due to small-scale but steep topographic variation (e.g., Edwards and Armbruster 1989; Zazula et al. 2003; Chytrý et al. 2019; Clarke et al. 2024). The observed variation could, however, reflect a subtle pattern related to microtopography. Studies of small-scale variation in both arctic tundra and dry steppe point to the possibility of features such as earth hummocks and local (sub-meter) disturbance of bare ground patches determining, for example, minimal but important differences in snow cover, nutrient availability, temperature and moisture that in turn relate to vegetation distribution (e.g., Martinez-Turanzas, Coffin, and Burke 1997; Khani et al. 2023). Smith et al. (1995) report earth hummocks developed on some modern surfaces of the Kolyma lowland, although whether these would be analogous to the MIS-3 surface is unclear. Also, the B3 sampling location was in a topographic low (Figure 5). Its taxon-rich samples that mix tundra forbs, grasses and more disturbance-related taxa (Figure 9) may reflect moisture in the depression plus local in-wash from the surrounding slopes, as loess can be highly mobile above and below ground.

Environmental change during MIS 2 and MIS 3

Anderson and Lozhkin (2001), Sher et al. (2005) and Murton et al. (2015) discussed the ambiguity of MIS 3 paleoclimatic conditions in western Beringia, underlining the poor dating control on older localities, upon

which the conventional interstadial sequence of two warm and two cool phases (between ca. 55,000 and 25,000 cal yr BP) is described. The evolving picture of MIS 3, based on more recent lacustrine records from the southern part of western Beringia (Lozhkin and Anderson 2011), is that there were several fluctuations in the abundance of trees and shrubs, suggesting alternations of warmer and colder intervals. Evidence is still sparse, however. In lacustrine records from Anadyr, there is evidence of moderately warm conditions ca. 35–31 ka BP, below a long hiatus marking the LGM (Lozhkin and Anderson 2013). In contrast, much farther north at El'gygytgyn Lake (Chukotka; Lozhkin et al. 2007), MIS-3 pollen assemblages indicate Poaceae–*Artemisia* tundra, probably with some *Salix*, and there is little difference between MIS-3 and MIS-2 assemblages.

Duvanny Yar loess is not without stratigraphic variation, but it is subtle. Several paleosols occur in lower parts of the section (lower than 25 m arl; Murton et al., 2015). In the sediments representing MIS 3 and 2, there is one paleosol, plus subtle color banding (see above). The key question is whether any of these variations reflect a response to regional climate conditions, whether they are related to small-scale landscape processes (e.g., varying loess accumulation patterns and the development of local topographic lows that may be moister than the surrounding surface), or, as suggested by Murton et al. (2015), they reflect regional changes but are only expressed on sensitive parts of the landscape. It is therefore worth comparing Duvanny Yar with other key sites in NE Siberia that predominantly feature yedoma ice-complex deposits.

In an earlier study at Duvanny Yar itself, Zanina et al. (2011) studied vertical profiles in outcrops exposed for ca. 9 km along the river; these profiles largely spanned MIS 3 and 2 in age. The sediment is dominated by cryopedolith (yedoma silt). Notably, these authors mapped several paleosol and peat layers along the length of the outcrop. The paleosols typically fall into ^{14}C age classes of ca. 38,000–35,000 (ca. 40,000 cal. yr BP); 33,000–30,000 (ca. 36,000 cal. yr BP; see above); and ca. 28,000 yr BP (ca. 31 cal. yr BP). Examination of the paleosols indicated dominant grass and forb (e.g. *Artemisia*) pollen, some *Betula* and *Salix* pollen and abundant moss spores, and plant macrofossils confirm that shrubs were locally present. Fossil rodent burrows, scattered in the MIS-3 yedoma silt at different positions between paleosols, yielded pollen, plant macrofossils, and insects. From their reported depths they probably largely reflect conditions during yedoma accumulation, not paleosol formation. Pollen spectra from burrows and surrounding sediments indicate an open environment, with taxa such as *Artemisia* and Caryophyllaceae, plus spores of mosses and fern allies (e.g., *Selaginella sibirica*). Plant macrofossils, however, included *Larix* seeds, and ecological affinities indicate a mosaic of communities: tundra, open larch woodland, poorly drained areas, disturbed areas, and steppe communities. The insect fauna, on the other hand, is clearly one of steppe–tundra, dominated by taxa such as *Morychus viridis* and *Stephanocladus eruditus*. It seems likely that the ground squirrels ranged across a landscape mosaic (see also Zazula et al. 2003 for a similar interpretation of squirrel-nest floras), while the insects reflect open communities, suggesting the wooded communities were more distant and/or rare. Our pollen data (partly a regional source) match those of Zanina et al. (2011), while the DNA flora aligns with the insect fauna (largely local sources). Zanina et al. (2011) hypothesized that the mosaic of communities and the sedimentation pattern of the paleosols can be explained by local warming triggering thawing in ice-wedge polygons. In contrast, the flora and fauna of MIS 2 indicate a more uniform steppe–tundra.

Sher et al. (2005) provided detailed data on sedimentology, insects, pollen and plant macrofossils from a large exposure on the Bykovsky Peninsula. Also based on baydzherakh sequences, it covers ca. 48,000 cal yr BP. The insect faunas are diverse but strongly dominated by taxa with xeric preferences. The pollen flora contains similar taxa to the flora in this study. The plant macrofossils (Sher et al. 2005; see also Keinast et al., 2001) suggest possible identities for poorly resolved taxa in pollen and *sed*aDNA. In the older part of the record, *Potentilla* cf. *stipularis, P. arenosa, Minuartia rubella*, and *Puccinellia distans* are, notably, representatives of genera found in this study; they indicate dry tundra, or even seasonally saline conditions. While composition changes subtly throughout the Bykovsky record, the main signal is of xerophilic taxa and dry tundra. Sher et al. (2005) also concluded that even quite marked features, such as a peat layer, most likely represent local landscape heterogeneity, rather than region-wide environmental change. For this area, Sher et al. (2005) and Wetterich et al. (2014) reconstructed a warmer early period, and then gradual temperature decline after ca. 35,000 cal yr BP.

In the New Siberian Islands, Andreev et al. (2009) described a series of sections, many of which cover the datable portion of MIS 3. The sections reveal multiple organic horizons, described as peat, or peaty soil, while the accompanying pollen data are highly consistent, being dominated by Poaceae and Cyperaceae, plus a rich and more varied range of forb taxa; this suggests that the organic layers likely reflect local dynamics, such

as the status of ice-wedge polygons. Plant macrofossils and insect faunas also support the notion of sparse steppe–tundra vegetation. The authors inferred a climatic deterioration (colder and drier) ca. 30,000 years ago, but unfortunately a hiatus interrupts the record shortly after this point.

At Batagay, in the highly continental Yana uplands, plant macrofossils in sediments dated to MIS 3 indicate predominantly meadow–steppe under dry conditions, with sparse *Larix* and occasional patches of tundra–steppe vegetation (Murton et al. 2023). In contrast to the other sites described above, steppe taxa dominate the MIS-3 period; however, MIS-2 conditions were more severe, as indicated by the abundant remains of *Morychus viridis* (see above).

In our Duvanny Yar pollen record, the diversity of forbs decreases, and the abundance of transported woody taxa increases toward and during MIS 2 (Fig. S2), suggesting sparser local vegetation that contributed less local pollen but continued to receive some regional pollen. Of *sed*aDNA taxa in the main section, Caryophyllaceae, *Anemone, Galium and Equisetum* are recorded only in MIS 3. *Elymus, Lemus, Tanacetum*, and *Eritrichium* are only recorded in MIS 2, the former three possibly suggesting more disturbed conditions, but it is an exceedingly subtle signal. Thus, the floristic record of MIS 3 and 2 at Duvanny Yar is largely unchanging across a period of hemispheric climate change, with only subtle evidence of declining growth conditions into MIS 2, and it suggests that xeric conditions persisted throughout the period. It is possible that the soil–vegetation system on interfluves dominated by loess fall —such as this Duvanny Yar site—may be more complacent in the face of environmental changes than, say, floodplains, or landscapes around lakes, two other sources of proxy information for this period.

The parsimonious explanation for the observed changes from MIS 3 to 2, expressed somewhat more clearly in some other studies than this one, is that growing conditions were driven largely by summer temperature, which dropped as northern hemisphere insolation declined, leading to a colder MIS 2 (Sher et al. 2005; Andreev et al. 2011). The general picture emerging from these sites is that MIS 3 saw some brief periods when either warmer (leading to thaw) or moister conditions allowed local organic accumulations and paleosol formation. From ca. 35,000 cal. yr BP onward, conditions became unrelentingly dry, with no major shifts or oscillations in climate during this period, apart from a gradual decline of summer temperature. Overall, the sites along the coastal zone of NE Siberia, including Duvanny Yar, show only subtle MIS-3 variability. Ideally, higher-resolution, regional proxy records of environmental change (e.g., stable isotopes, biomarkers, pollen) are needed to make a clear comparison with southern portions of western Beringia.

Conclusion

Of the major studied exposures of the Yedoma Ice Complex landscapes of NE Siberia, this Duvanny Yar locality, despite an excellent radiocarbon chronology, is perhaps the most enigmatic in terms of its climatological and biotic records, in that it shows remarkably little variation during MIS 3 and 2. Nevertheless, the *sed*aDNA and pollen data paint a coherent picture of the MIS 2 and 3 flora at Duvanny Yar, reinforcing each other to indicate treeless, grass–forb-dominated vegetation, which aligns with the mammalian DNA, the regional mammalian fossil-bone record and pollen, macrofossil and insect data from other sites. Molecular taxon frequencies and modified read abundances suggest a ca. 50–50 split, or possibly a slightly greater dominance of forbs over grasses, but whether this accurately reflects biomass (above- or below-ground) is a question that requires further investigation, and the magnitude of the biomass represented remains a key unanswered question in Beringian paleoecology. Floristically, the data align most closely with vegetation types such as cold steppe or dry tundra, probably with considerable levels of disturbance. Within the limited spatial scope of the study, only subtle topographic changes are seen in the paleo-landscape during MIS 3. Fine-scale vegetation spatial heterogeneity is most likely related to microtopography. We conclude that *sed*aDNA from yedoma has great potential to provide further information on the ancient Beringian ecosystems of MIS 3 and 2 but note that at any given point, the flora is likely under-sampled and the age will carry some uncertainty. A combination of horizontal and vertical sampling could reduce uncertainty on both counts. With the continued improvement of molecular approaches, there is great potential for well dated, high-resolution regional to further resolve floristic, faunal and paleoenvironmental records for the Beringia.

Acknowledgments

We thank Piotr Danilov, James Haile, Tina Jorgensen, David Alquezar, and Alexei Tikhonov for their efforts in the field, and Sergey, Nikolai, and Natasha Zimov for logistic support in the field and at Cherskiy Field Station. Gregorii Savinov also supported the field team. The late

Stas Gubin provided JM with helpful advice on yedoma. Scott Armbruster contributed thoughtful ideas regarding palaeoecological interpretation. H.M. and Y.W. were supported by the NSFC BSCTPES Project (No. 41988101), the CAS Youth Interdisciplinary Team Fund, the Carlsberg Foundation (CF18-0024), the Danish National Research Foundation (DNRF174), and the Novo Nordisk Foundation (NNF24SA0092560). Shotgun data analysis was supported by the National Key Scientific and Technological Infrastructure project "Earth System Numerical Simulation Facility" (EarthLab, 2023-EL-ZD -000111) and SMU's Center for Research Computing. Original fieldwork and sample analysis (MEE and JM) was funded by ECOCHANGE (EU grant GOCE-2006-036866). The team who initially dated, processed and archived the samples and data that are re-used in this study are Heather Binney, Eric Coissac, Ludovic Gielly, Tomasz Goslar, James Haile and Mari Moora. Christian Brochmann, Pierre Taberlet and Eske Willerslev were the PIs of ECOCHANGE.

Disclosure statement

No potential conflict of interest was reported by the author(s).

Funding

This work was supported by the Carlsbergfondet [CF18-0024]; Danmarks Grundforskningsfond [DNRF174]; EarthLab [2023-EL-ZD-000111]; Novo Nordisk Foundation [(NNF24SA0092560]; NSFC BSCTPES [41988101]; Sixth Framework Programme [GOCE-2006-036866].

ORCID

Mary Edwards http://orcid.org/0000-0002-3490-6682

Dedication

This article is dedicated to the memory of Stanislav Gubin, who died in 2025—the year of his 80th birthday. Stas worked for many decades on Duvanny Yar and other sites in NE Siberia, and he has greatly increased our knowledge of the paleopedology of yedoma. Stas was a key member of the Russian team that engaged in the first joint work between Russian and U.S. scientists (including MEE) in 1990–1991 during the era of open cooperation, and he was also instrumental in advising the 2009 ECOCHANGE field team in Cherskiy.

Data availability statement

The original DNA data as reported in Willerslev et al. (2014) can be found at https://www.nature.com/articles/nature12921#Sec37. For original shotgun data reported in Wang et al. (2021) see https://www.ebi.ac.uk/ena/browser/view/PRJEB43822.

The molecular datasets and the pollen data used in this study and the complete OxCal v.4.4.4 code are available in the SI.

References

Alfimov, A.V., D.I. Berman, and A.V. Sher. 2003. Tundra-steppe insect assemblages and reconstructions of late Pleistocene climate in the lower reaches of the Kolyma River [in Russian]. *Zoologicheskiy Zhurnal* 82: 281–300.

Alsos, I.G., Y. Lammers, N.G. Yoccoz, T. Jørgensen, P. Sjögren, L. Gielly, and M.E. Edwards. 2018. Plant DNA metabarcoding of lake sediments: How does it represent the contemporary vegetation? *PLOS ONE* 13, no. 4: e0195403. doi:10.1371/journal.pone.0195403.

Alsos, I.G., P. Sjögren, M.E. Edwards, J.Y. Landvik, L. Gielly, M. Forwick, E. Coissac, et al. 2016. Sedimentary ancient DNA from Lake Skartjørna, Svalbard: Assessing the resilience of Arctic flora to Holocene climate change. *The Holocene* 26, no. 4: 627–42. doi:10.1177/095968361561256.

Anderson, P.M., and A.V. Lozhkin. 2001. The stage 3 interstadial complex (Karginskii/middle Wisconsinan interval) of Beringia: Variations in paleoenvironments and implications or paleoclimatic interpretations. *Quaternary Science Reviews* 20: 93–125. doi:10.1016/S0277-3791(00)00129-3.

Andreev, A. A., G. Grosse, L. Schirrmeister, T. V. Kuznetsova, S. A. Kuzmina, A. A. Bobrov, P. E. Tarasov, et al. 2009. Weichselian and holocene palaeoenvironmental history of the Bol'shoy Lyakhovsky Island, new Siberian archipelago, Arctic Siberia. *Boreas* 38, no. 1: 72–110. doi:10.1111/j.1502-3885.2008.00039.x.

Andreev, A. A., L. Schirrmeister, P. E. Tarasov, A. Ganopolski, V. Brovkin, C. Siegert, S. Wetterich, and H. W. Hubberten. 2011. Vegetation and climate history in the Laptev Sea region (Arctic Siberia) during late quaternary inferred from pollen records. *Quaternary Science Reviews* 30, no. 17–18: 2182–99. doi:10.1016/j.quascirev.2010.12.026.

Arnold, L.J., R.G. Roberts, R.D. Macphee, J.S. Haile, F. Brock, P. Möller, D.G. Froese, et al. 2011. Paper II–dirt, dates and DNA: OSL and radiocarbon chronologies of perennially frozen sediments in Siberia, and their implications for sedimentary ancient DNA studies. *Boreas* 40, no. 3: 417–45. doi:10.1111/j.1502-3885.2010.00181.x.

Boeskorov, G.G., O.R. Potapova, A.V. Protopopov, V. V. Plotnikov, E.N. Maschenko, M.V. Shchelchkova, E. A. Petrova, R. Kowalczyk, J. van der Plicht, and A. N. Tikhonov. 2018. A study of a frozen mummy of a wild horse from the Holocene of Yakutia, East Siberia, Russia. *Mammal Research* 63, no. 3: 307–14. doi:10.1007/s13364-018-0362-4.

Boessenkool, S., L.S. Epp, E.V.A.B. James Haile, M. Edwards, E. Coissac, E. Willerslev, and C. Brochmann. 2012. Blocking human contaminant DNA during PCR allows amplification of rare mammal species from sedimentary ancient DNA. *Molecular Ecology* 21, no. 8: 1806–15. doi:10.1111/j.1365-294X.2011.05306.x.

Bronk Ramsey, C.B. 2008. Deposition models for chronological records. *Quaternary Science Reviews* 27: 42–60. doi:10.1016/j.quascirev.2007.01.019.

Bronk Ramsey, C.B. 2009. Bayesian analysis of radiocarbon dates. *Radiocarbon* 51, no. 1: 337–60. doi:10.1017/S0033822200033865.

Chen, S., Y. Zhou, Y. Chen, and J. Gu. 2018. Fastp: An ultra-fast all-in-one FASTQ preprocessor. *Bioinformatics* 34, no. 17: i884–i890. doi:10.1093/bioinformatics/bty560.

Chytrý, M., M. Horsák, J. Danihelka, N. Ermakov, D. A. German, M. Hájek, P. Hájková, et al. 2019. A modern analogue of the Pleistocene steppe-tundra ecosystem in southern Siberia. *Boreas* 48, no. 1: 36–56. doi:10.1111/bor.12338.

Clarke, C., M. Edwards, N. Bigelow, P. Heinzman, B. Potter, I. Alsos, and J. Reuther. 2021. Late Quaternary vegetation dynamics in interior Alaska revealed by sedimentary ancient DNA (*sedaDNA*) from lake sediment and unfrozen (loessic) archaeological sediments. Online Abstract session EGU21-13501, EGU (2021).

Clarke, C.L., M.E. Edwards, L. Gielly, D. Ehrich, P.D. M. Hughes, L.M. Morozova, H. Haflidason, J. Mangerud, J.I. Svendsen, and I.G. Alsos. 2019. Persistence of Arctic-alpine flora during 24,000 years of environmental change in the Polar Urals. *Scientific Reports* 9, no. 1: 19613. doi:10.1038/s41598-019-55989-9.

Clarke, C.L., P.D. Heintzman, Y. Lammers, A.J. Monteath, N. H. Bigelow, J.D. Reuther, B.A. Potter, P.D. Hughes, I. G. Alsos, and M.E. Edwards. 2024. Steppe-tundra composition and deglacial floristic turnover in interior Alaska revealed by sedimentary ancient DNA (*sedaDNA*). *Quaternary Science Reviews* 334: 108672. doi:10.1016/j.quascirev.2024.108672.

Courtin, J., A. Perfumo, A.A. Andreev, T. Opel, K.R. Stoof-Leichsenring, M.E. Edwards, J.B. Murton, and U. Herzschuh. 2022. Pleistocene glacial and interglacial ecosystems inferred from ancient DNA analyses of permafrost sediments from Batagay megaslump, East Siberia. *Environmental DNA* 4, no. 6: 1265–83. doi:10.1002/edn3.336.

Edwards, M.E., I.G. Alsos, N. Yoccoz, E. Coissac, T. Goslar, L. Gielly, J. Haile, et al. 2018. Metabarcoding of modern soil DNA gives a highly local vegetation signal in Svalbard tundra. *Holocene* 28, no. 12: 2006–16. doi:10.1177/0959683618798095.

Edwards, M.E., and W.S. Armbruster. 1989. A tundra-steppe transition on Kathul Mountain, Alaska, USA. *Arctic and Alpine Research* 21, no. 3: 296–304. doi:10.1080/00040851.1989.12002742.

Epp, L.S., S. Boessenkool, E.P. Bellemain, J. Haile, A. Esposito, T. Riaz, C. Erseus, et al. 2012. New environmental metabarcodes for analysing soil DNA: Potential for studying past and present ecosystems. *Molecular Ecology* 21, no. 8: 1821–33. doi:10.1111/j.1365-294X.2012.05537.x.

Ficetola, G.F., J. Pansu, A. Bonin, E. Coissac, C. Giguet-Covex, M. De Barba, L. Gielly, et al. 2015. Replication levels, false presences and the estimation of the presence/absence from eDNA metabarcoding data. *Molecular Ecology Resources* 15, no. 3: 543–56. doi:10.1111/1755-0998.12338.

Fordman, D.A., S.C. Brown, E. Canteri, J.J. Austin, M. V. Lomolino, S. Haythorne, E. Armstrong, et al. 2024. 52,000 years of woolly rhinoceros population dynamics reveal extinction mechanisms. *Proceedings of the National Academy of Sciences* 121, no. 24: e2316419121. doi:10.1073/pnas.2316419121.

Freeman, C.L., L. Dieudonné, O.B.A. Agbaje, M. Žure, J. Q. Sanz, M. Collins, and K.K. Sand. 2023. Survival of environmental DNA in sediments: Mineralogic control on DNA taphonomy. *Environmental DNA* 5, no. 6: 1691–705. doi:10.1002/edn3.482.

Giguet-Covex, C., G.F. Ficetola, K. Walsh, J. Poulenard, M. Bajard, L. Fouinat, P. Sabatier, et al. 2019. New insights on lake sediment DNA from the catchment: Importance of taphonomic and analytical issues on the record quality. *Scientific Reports* 9, no. 1: 14676. doi:10.1038/s41598-019-50339-1.

Grimm, E.C. 1992. Tilia and tilia-graph: Pollen spreadsheet and graphics programs. In *Programs and abstracts, 8th International Palynological Congress*, Aix-en-Provence. September 6-12, 1992. 56.

Gubin, S.V. 2002. Pedogenesis—the main component of the late Pleistocene ice complex forming [in Russian]. *Earth Cryosphere* 6: 82–91.

Gubin, S.V., and A.V. Lupachev. 2008. Soil formation and the underlying permafrost. *Eurasian Soil Science* 41, no. 6: 574–85. doi:10.1134/S1064229308060021.

Gubin, S.V., and A.A. Veremeeva. 2010. Parent materials enriched in organic matter in the northeast of Russia. *Eurasian Soil Science* 43, no. 11: 1238–43. doi:10.1134/S1064229310110062.

Guthrie, R.D. 1990. *Frozen fauna of the Mammoth Steppe: The story of Blue Babe*. Chicago: University of Chicago Press.

Guthrie, R.D. 2001. Origin and causes of the mammoth steppe: A story of cloud cover, woolly mammal tooth pits, buckles, and inside-out Beringia. *Quaternary Science Reviews* 20, no. 1: 549-74.

Hammer, Ø., D.A.T. Harper, and P.D. Ryan. 2001. Past: Paleontological statistics software package for education and data analysis. *Paleontologia Electronica* 4, no. 1: 9.

Hopkins, D.M. 1982. Aspects of the paleogeography of Beringia during the late Pleistocene. In *Paleoecology of Beringia* (D. M Hopkins, J.V. Matthews, Jr, and C.E. Schweger, S. B Young, Eds.), 3–28. New York: Academic Press.

Jacobsen, G.L., and R.H.W. Bradshaw. 1981. The selection of sites for palaeovegetational studies. *Quaternary Research* 16, no. 1: 80–96. doi:10.1016/0033-5894(81)90129-0.

Jónsson, H., A. Ginolhac, M. Schubert, P.L. Johnson, and L. Orlando. 2013. Fast approximate Bayesian estimates of ancient DNA damage parameters. *Bioinformatics*29, no. 13: 1682–4. doi: 10.1093/bioinformatics/btt193.

Jorgensen, T., J. Haile, P. Moller, A. Andreev, S. Boessenkool, M. Rasmussen, F. Kienast, et al. 2012. A comparative study of ancient sedimentary DNA, pollen and macrofossils from permafrost sediments of northern Siberia reveals long-term vegetational stability. *Molecular Ecology* 21, no. 8: 1989–2003. doi:10.1111/j.1365-294X.2011.05287.x.

Kaplina, T.N., G. RYe, O.V. Lakhtina, B.A. Abrashov, and A. V. Sher. 1978. Duvanny Yar, a key section of upper Pleistocene sediments of the Kolyma lowland. *Bulletin of the Commission of the USSR Academy of Sciences for studying the Quaternary* [in Russian]. 48: 49–65.

Khani, H.M., C. Kinnard, S. Gascoin, and E. Lévesque. 2023. Finescale environment control on ground surface temperature and thaw depth in a high arctic tundra landscape. *Permafrost and Periglacial Processes* 34, no. 4: 467–80. doi:10.1002/ppp.2203.

Kienast, F., C. Siegert, A.Y. Derevyagin, and H.D. Mai. 2001. Climatic implications of late Quaternary plant macrofossil assemblages from the Taimyr Peninsula, Siberia. *Global and*

Planetary Change 31, no. 1–4: 265–81. doi:10.1016/S0921-8181(01)00124-2.

Kuznetsova, T.V., S. Wetterich, H. Matthes, V.E. Tumskoy, and L. Schirrmeister. 2022. Mammoth fauna remains from late Pleistocene deposits of the Dmitry Laptev Strait south coast (northern Yakutia, Russia). *Frontiers in Earth Science* 10: 757629. doi:10.3389/feart.2022.757629.

Laschinskiy, N., A. Faguet, and C. Biasi, 2020. Primary plant succession on freshly degraded yedoma (ice complex) in Lena Delta (Eastern Siberia). In *BIO Web of Conferences* (Vol. 24, p. 00047). EDP Sciences.

Laxton, N.F., C.R. Burn, and C.A.S. Smith. 1996. Productivity of loessal grasslands in the Kluane Lake region, Yukon Territory, and the Beringian "production paradox." *Arctic* 49, no. 2: 129–140. doi:10.14430/arctic1191.

Li, H., B. Handsaker, A. Wysoker, T. Fennell, J. Ruan, N. Homer, G. Marth, G. Abecasis, R. Durbin and 1000 Genome Project Data Processing Subgroup. 2009. *The Sequence Alignment/Map Format and SAMtools. Bioinformatics* 25, no. 16: 2078–9.

Lozhkin, A.V., and P.M. Anderson. 2011. Forest or no forest: Implications of the vegetation record for climatic stability in western Beringia during oxygen isotope stage 3. *Quaternary Science Reviews* 30, no. 17–18: 2160–81. doi:10.1016/j.quascirev.2010.12.022.

Lozhkin, A.V., and P.M. Anderson. 2013. Late quaternary lake records from the Anadyr lowland, central Chukotka (Russia). *Quaternary Science Reviews* 68: 1–16. doi:10.1016/j.quascirev.2013.02.007.

Lozhkin, A.V., and P.M. Anderson. 2016. About the age and habitat of the Kirgilyakh mammoth (Dima), Western Beringia. *Quaternary Science Reviews* 145: 104–16. doi:10.1016/j.quascirev.2016.05.028.

Lozhkin, A.V., P.M. Anderson, T.V. Matrosova, and P. S. Minyuk. 2007. The pollen record from El'gygytgyn Lake: Implications for vegetation and climate histories of northern Chukotka since the late middle Pleistocene. *Journal of Paleolimnology* 37, no. 1: 135–53. doi:10.1007/s10933-006-9018-5.

Lupachev, A.V., N.I. Tananaev, J.B. Murton, P.I. Kalinin, V. V. Malyshev, and P.P. Danilov. 2025. Microstructure and geochemical properties of modern and buried soils and hosting permafrost sediments of the Batagay retrogressive thaw slump. *Quaternary Research* 125: 35–55. doi:10.1017/qua.2024.58.

Martin, P.S. 1984. Prehistoric overkill: The global model. In *Quaternary extinctions: a prehistoric revolution*, ed. P. S. Martin and R.G. Klein, 354–403. University of Arizona Press.

Martinez-Turanzas, G.A., D.P. Coffin, and I.C. Burke. 1997. Development of microtopography in a semi-arid grassland: Effects of disturbance size and soil texture. *Plant & Soil* 191, no. 2: 163–71. doi:10.1023/A:1004286605052.

Meyer, M., and M. Kircher. 2010. Illumina sequencing library preparation for highly multiplexed target capture and sequencing. *Cold Spring Harbor Protocols* 2010, no. 6: 5448. doi:10.1101/pdb.prot5448.

Monteath, A.J., M.E. Edwards, D. Froese, L. Anderson, B. V. Gaglioti, S.L. Cocker, J. Brigham-Grette, M.J. Wooller, B. Finney, and M.B. Abbott. 2025. Late Quaternary environmental change in eastern Beringia: New advances and unresolved questions. *Quaternary Science Reviews* 368, no. 2025: 109527.

Monteath, A.J., S. Kuzmina, M. Mahony, F. Calmels, T. Porter, R. Mathewes, P. Sanborn, et al. 2023. Relict permafrost preserves megafauna, insects, pollen, soils and pore-ice isotopes of the mammoth steppe and its collapse in central Yukon. *Quaternary Science Reviews* 299: 107878.

Murchie, T.J., M. Kuch, A.T. Duggan, M.L. Ledger, K. Roche, J. Klunk, E. Karpinski, et al. 2021b. Optimizing extraction and targeted capture of ancient environmental DNA for reconstructing past environments using the PaleoChip Arctic-1.0 bait-set. *Quaternary Research* 99: 305–28. doi:10.1017/qua.2020.59.

Murchie, T.J., G.S. Long, B.D. Lanoil, D. Froese, and H. N. Poinar. 2023. Permafrost microbial communities follow shifts in vegetation, soils, and megafauna extinctions in late Pleistocene NW North America. *Environmental DNA* 5, no. 6: 1759–79. doi:10.1002/edn3.493.

Murchie, T.J., A.J. Monteath, M.E. Mahony, G.S. Long, S. Cocker, T. Sadoway, E. Karpinski, et al. 2021a. Collapse of the mammoth-steppe in central Yukon as revealed by ancient environmental DNA. *Nature Communications* 12, no. 1: 7120. doi:10.1038/s41467-021-27439-6.

Murton, J.B., T. Goslar, M.E. Edwards, M.D. Bateman, P. P. Danilov, G.N. Savvinov, S.V. Gubin, et al. 2015. Paleoenvironmental interpretation of Yedoma silt (ice complex) deposition as cold-climate loess, Duvanny Yar, northeast Siberia. *Permafrost and Periglacial Processes* 26, no. 3: 208–88. doi: 10.1002/ppp.1843.

Murton, J.B. 2022a. Ground ice. In *Treatise on geomorphology*, ed. and J. Shroder, vol. 4. 2nd ed. 428–57. San Diego, CA: Academic Press.

Murton, J.B. 2022b. Cryostratigraphy. In *Treatise on geomorphology*, ed. J. Shroder, vol. 4. 2nd ed., 458–90. San Diego, CA: Academic Press.

Murton, J., T. Opel, S. Wetterich, K. Ashastina, G. Savvinov, P. Danilov, and V. Boeskorov. 2023. Batagay megaslump: A review of the permafrost deposits, Quaternary environmental history, and recent development. *Permafrost and Periglacial Processes* 34, no. 3: 399–416. doi:10.1002/ppp.2194.

PALE Steering Committee. 1994. Research protocols for PALE: Paleoclimate of Arctic Lakes and Estuaries, PAGES workshop report series 94-1. PAGES Core Project Office: Bern.

Parducci, L., I.G. Alsos, P. Unneberg, M.W. Pedersen, L. U. Han, Y. Lammers, J.S. Salonen, M.M. Väliranta, T. Slotte, and B. Wohlfarth. 2019. Shotgun environmental DNA, pollen, and macrofossil analysis of lateglacial lake sediments from southern Sweden. *Frontiers in Ecology and Evolution* 7: 189. doi:10.3389/fevo.2019.00189.

Park, H., T. Yamazaki, K. Yamamoto, and T. Ohta. 2008. Tempo-spatial characteristics of energy budget and evapotranspiration in the eastern Siberia. *Agricultural and Forest Meteorology* 148, no. 12: 1990–2005. doi:10.1016/j.agrformet.2008.06.018.

Pedersen, M.W., A. Ruter, C. Schweger, H. Friebe, R.A. Staff, K.K. Kjeldsen, M.L. Mendoza, et al. 2016. Postglacial viability and colonization in North America's ice-free corridor. *Nature* 537, no. 7618: 45–9. doi:10.1038/nature19085.

Péwé, T.L., and A. Journaux 1983. Origin and character of loess-like silt in unglaciated southcentral Yakutia, Siberia,

U.S.S.R. United States Geological Survey professional paper 1262, Washington, DC.

Prentice, I.C. 1985. Pollen representation, source area, and basin size: Toward a unified theory of pollen analysis. *Quaternary Research* 23, no. 1: 76–86. doi:10.1016/0033-5894(85)90073-0.

Reimer, P.J., W.E. Austin, E. Bard, A. Bayliss, P.G. Blackwell, C.B. Ramsey, M. Butzin, et al. 2020. The IntCal20 Northern Hemisphere radiocarbon age calibration curve (0–55 cal kBP). *Radiocarbon* 62, no. 4: 725–57. doi:10.1017/RDC.2020.41.

Schirrmeister, L., E. Dietze, H. Matthes, G. Grosse, J. Strauss, S. Laboor, M. Ulrich, F. Kienast, and S. Wetterich. 2020. The genesis of Yedoma Ice Complex permafrost – grain-size endmember modeling analysis from Siberia and Alaska. *E&G Quaternary Science Journal* 69, no. 1: 33–53. doi:10.5194/egqsj-69-33-2020.

Schirrmeister, L., D. Froese, S. Wetterich, et al. 2025. Yedoma: Late Pleistocene ice-rich syngenetic permafrost of Beringia. In *Encyclopedia of Quaternary Science*, ed. S. Elias. Vol. 5 296–311, Elsevier.

Seeber, P.A., L. Batke, Y. Dvornikov, A. Schmidt, Y. Wang, K. Stoof-Leichsenring, K. Moon, S.H. Vohr, B. Shapiro, and L.S. Epp. 2024. Mitochondrial genomes of Pleistocene megafauna retrieved from recent sediment layers of two Siberian lakes. *Elife* 12: 89992. doi:10.7554/eLife.89992.3.

Sher, A.V., T.N. Kaplina, R.E. Giterman, A.V. Lozhkin, A. A. Arkhangelov, S.V. Kiselyov, Y.V. Kouznetsov, E. I. Virina, and V.S. Zazhigin. 1979. *Late Cenozoic of the Kolyma Lowland: XIV Pacific Science Congress, Khabarovsk August 1979, tour guide XI*, 1–116. Moscow: USSR Academy of Sciences.

Sher, A.V., and S.A. Kuzmina. 2007. Beetle records. Late Pleistocene of northern Asia.. In *Encyclopedia of quaternary science*, ed. S.A. Elias. Vol. 1 246–67. Elsevier.

Sher, A.V., S.A. Kuzmina, T.V. Kuznetsova, and L. D. Sulerzhitsky. 2005. New insights into the Weichselian environment and climate of the East Siberian Arctic, derived from fossil insects, plants, and mammals. *Quaternary Science Reviews* 24, no. 5–6: 533–69. doi:10.1016/j.quascirev.2004.09.007.

Shur, Y., K.M. Hinkel, and F.E. Nelson. 2005. The transient layer: Implications for geocryology and climate-change science. *Permafrost and Periglacial Processes* 16, no. 1: 5–18. doi:10.1002/ppp.518.

Shur, Y.L. 1988. *Upper horizon of permafrost and thermokarst*. Nauka: Novosibirsk (in Russian).

Smith, C.A.S., D.K. Swanson, J.P. Moore, J.P. Ahrens, J. G. Bockheim, J.M. Kimble, G.G. Mazhitova, C.L. Ping, and C. Tarnocai. 1995. A description and classification of soils and landscapes of the lower Kolyma River, northeastern Russia. *Polar Geography and Geology* 19, no. 2: 107–26. doi:10.1080/10889379509377563.

Strauss, J., S. Laboor, L. Schirrmeister, et al. 2021. Circum-Arctic map of the Yedoma permafrost domain. *Frontiers in Earth Science* 9: 758360. doi:10.3389/feart.2021.758360.

Strauss, J., L. Schirrmeister, S. Wetterich, A. Borchers, and S. P. Davydov. 2012. Grain-size properties and organic-carbon stock of Yedoma Ice Complex permafrost from the Kolyma lowland, Northeastern Siberia. *Global Biogeochemical Cycles* 26, no. 3. doi:10.1029/2011GB004104

Taberlet, P., E. Coissac, F. Pompanon, L. Gielly, C. Miquel, A. Valentini, T. Vermat, G. Corthier, C. Brochmann, and E. Willerslev. 2007. Power and limitations of the chloroplast trnL (UAA) intron for plant DNA barcoding. *Nucleic Acids Research* 35, no. 3: e14. doi:10.1093/nar/gkl938.

Taberlet, P., S.M. Prud'Homme, E. Campione, J. Roy, C. Miquel, W. Shehzad, L. Gielly, et al. 2012. Soil sampling and isolation of extracellular DNA from large amount of starting material suitable for metabarcoding studies. *Molecular Ecology* 21, no. 8: 1816–20. doi:10.1111/j.1365-294X.2011.05317.x.

Ulrich, M., G. Grosse, J. Stauss, and L. Schirrmeister. 2014. Quantifying wedge-ice volumes in yedoma and thermokarst basin deposits. *Permafrost and Periglacial Processes* 25, no. 3: 151–61. doi:10.1002/ppp.1810.

Wang, Y., M.W. Pedersen, I.G. Alsos, B. De Sanctis, F. Racimo, A. Prohaska, E. Coissac, et al. 2021. Late Quaternary dynamics of Arctic biota from ancient environmental genomics. *Nature* 600, no. 7887: 86–92. doi:10.1038/s41586-021-04016-x.

Wetterich, S., N. Rudaya, V. Tumskoy, A.A. Andreev, T. Opel, L. Schirrmeister, and H. Meyer. 2011. Last glacial maximum records in permafrost of the East Siberian Arctic. *Quaternary Science Reviews* 30, no. 21–22: 3139–51. doi:10.1016/j.quascirev.2011.07.020.

Wetterich, S., V. Tumskoy, N. Rudaya, A.A. Andreev, T. Opel, H. Meyer, L. Schirrmeister, and M. Hüls. 2014. Ice complex formation in Arctic East Siberia during the MIS3 interstadial. *Quaternary Science Reviews* 84: 39–55. doi:10.1016/j.quascirev.2013.11.009.

Willerslev, E., J. Davison, M. Moora, M. Zobel, E. Coissac, M. E. Edwards, E.D. Lorenzen, et al. 2014. Fifty thousand years of Arctic vegetation and megafaunal diet. *Nature* 506, no. 7486: 47–51. doi:10.1038/nature12921.

Willerslev, E., A.J. Hansen, J. Binladen, T.B. Brand, M.T. P. Gilbert, B. Shapiro, M. Bunce, C. Wiuf, D. A. Gilichinsky, and A. Cooper. 2003. Diverse plant and animal genetic records from Holocene and Pleistocene sediments. *Science* 300, no. 5620: 791–5. doi:10.1126/science.1084114.

Yoccoz, N.G., K.A. Bråthen, L. Gielly, J. Haile, M.E. Edwards, T. Goslar, H. von Stedingk, et al. 2012. Dna from soil mirrors plant taxonomic and growth form diversity. *Molecular Ecology* 21, no. 15: 3647–55. doi:10.1111/j.1365-294X.2012.05545.x.

Yurtsev, B.A. 1982. Relics of the xerophyte vegetation of Beringia in northeastern Asia. In *Paleoecology of Beringia*, eds. J.V. Hopkins, C.E. Matthews, and S.B.Y. Schweger, 157–77. San Diego: Academic Press.

Zanina, O.G. 2005. Fossil rodent burrows in frozen late Pleistocene beds of the Kolyma lowland. *Entomological Review* 85, no. Supplement1: 133–40.

Zanina, O.G., S.V. Gubin, S.A. Kuzmina, S.V. Maximovich, and D.A. Lopatina. 2011. Late-Pleistocene (MIS 3-2) paleoenvironments as recorded by sediments, paleosols, and ground-squirrel nests at Duvanny Yar, Kolyma lowland, northeast Siberia. *Quaternary Science Reviews* 30, no. 17–18: 2107–23. doi:10.1016/j.quascirev.2011.01.021.

Zazula, G.D., D.G. Froese, C.E. Schweger, R.W. Mathewes, A. B. Beaudoin, A.M. Telka, C.R. Harington, and J.A. Westgate. 2003. Ice-age steppe vegetation in East Beringia. *Nature* 423, no. 6940: 603–603. doi:10.1038/423603a.

Zimmermann, H.H., E. Raschke, L.S. Epp, K.R. Stoof-Leichsenring, G. Schwamborn, G. Schwamborn, U. Herzchuh, and U. Herzschuh. 2017. Sedimentary ancient DNA and pollen reveal the composition of plant organic matter in late Quaternary permafrost sediments of the Buor Khaya Peninsula (north-eastern Siberia). *Biogeosciences* 14, no. 3: 575–96. doi:10.5194/bg-14-575-2017.